

**Wettability of Nanofibrous Membrane Regulating Stem Cell
Differentiation**

by

Haiyun Gao

A Thesis submitted to the Faculty of Graduate Studies of

The University of Manitoba

in partial fulfilment of the requirements of the degree of

MASTER OF SCIENCE

Department of Textile Sciences

University of Manitoba

Winnipeg

Copyright © 2012 by Haiyun Gao

Content

Abstract	V
Acknowledgement	VI
List of Tables	VII
List of Figures	VIII
Chapter I: Introduction.....	1
1.1 Background.....	1
1.2 Hypothesis and objectives.....	2
Chapter II: Literature Review	4
2.1 Cell-niche interactions and <i>in vitro</i> recapitulation.....	5
2.2 Biochemical cues regulate stem cell fate	6
2.3 Cell shape regulates stem cell fate	8
2.4 Biophysical cues regulate stem cell fate	10
2.5 Nano-biosystem interface regulate stem cell fate	13
Chapter III: Materials and Methods.....	15
3.1 Materials	15
3.2 Fabrication of electrospun nanofibrous membranes	15
3.3 Characterization of nanofibres	16
3.3.1 Contact angle measurement	16
3.3.2 IR-ATR spectroscopic analyses	17
3.3.3 <i>In vitro</i> degradation.....	17
3.3.4 XPS characterization.....	17

3.4 Cell culture.....	18
3.5 Scanning Electron Microscopy (SEM) for substrate and cell morphological examination.....	18
3.6 Cell viability study.....	19
3.7 Real-Time PCR.....	20
3.7.1 Cell lines and treatment	20
3.7.2 Quantitative Real-time PCR analysis.....	20
3.7.3 Western Blot Analysis	21
3.8 Statistical analysis	22
Chapter IV: Results and Discussion	23
4.1 Design of tunable matrices with varying wettability	23
4.2 Characterization of composite nanofibres	25
4.3 In vitro degradation tests of the nanofibrous membranes	29
4.4 Matrices hydrophobicity-mediated cell adhesion and proliferation of MSCs.....	31
4.5 Cell viability on nanofibrous membranes	35
4.6 Changes in mRNA expression of MSCs in bone-derived scaffolds made from different nano-membranes	37
4.7 Involvement of ERK1/2 activation in membranes that promote osteogenesis	39
4.8 The relationship between MSCs' osteogenic differentiation on different nano-membrane.....	41
4.9 Nano-membrane stimulation of MSCs' osteogenic differentiation through ERK1/2 signaling pathways.....	43
Chapter V: Conclusions and Future Studies	44

References.....	46
-----------------	----

Abstract

In this work, I investigated the influence of different surfaces on stem cell proliferation and osteogenetic differentiation. Surface properties of biomaterials are important factors that influence cell fate such as cell adhesion, viability, proliferation and differentiation. Herein, mesenchymal stem cells (MSCs) were cultured on composite electrospun nanofibrous membranes with varied surface wettability for designed periods and cell morphologies, proliferation and viability were characterized via analysis methods such as Infrared attenuated total reflectance Spectroscopy (IR-ATR), scanning electron microscopy (SEM) and MTT cell proliferation assay. The expression of genes associated with osteogenesis, including bone sialoprotein (BSP), alkaline phosphatase (ALP), osteopontin (OPN) and osteocalcin (OCN) were measured by real-time RT-PCR on different time points. Through western blot analysis, ERK1/2 pathway was found to be responsible for the differentiation of MSCs on nanofibrous membranes with different wettability.

Acknowledgement

I would like first to thank Dr. Malcolm Xing, Dr. Wen Zhong (my supervisors) and Dr. Leyu Wang for their guidance, encouragement, support and good advice.

Second I would like to thank my thesis committee, Dr. Martin King and Dr. Ying Chen, for their direction and invaluable advice for my thesis.

My heartfelt acknowledgement also goes to Dr. Jun Chen, who has been abundantly helpful and providing many great advices. I specially thank him for his infinite patience. The discussions I had with him were invaluable.

I am grateful to all my colleagues for being the surrogate family during the two years I stayed in Winnipeg and for their continued love and support.

My final words go to my family. I want to thank my family, whose love and guidance is with me in whatever I pursue.

On a different note, many people have been a part of my graduate education and I am highly grateful to all of them.

List of Tables

Table 1 Sequences of primers for the qRT-PCR	21
Table 2 Contact angle measurement of gelatin/PCL (G/P) nanofibres.....	23

List of Figures

Figure 1 Contact angles of different electrospun fibrous membranes. From pure PCL (most left column) to pure gelatin (most right column) the membranes show a significant decrease in water contact angle, indicating a gradual decreasing trend in wettability.	23
Figure 2 Characterization of nanofibres. (A) IR-ATR spectroscopic analysis of non-crosslinked gelatin/PCL nanofibrous membranes. (B-E) XPS analysis of nanofibres without crosslinking. (B, G10P0; C, G7P3; D, G3P7; E, G0P10)	26
Figure 3 Degradation tests of gelatin/PCL nanofibrous membranes in (A) PBS and (B) cell culture medium for 1, 4 and 7 days. Bars indicate the mean values for all measured nanofibrous membranes, n = 5.	29
Figure 4 SEM micrographs of (A) gelatin (G10P0), gelatin/PCL (G7P3, G3P7) and PCL (G0P10) nanofibrous scaffolds (left to right); (B) MSCs on different nanofibrous scaffolds after 24hr of cultivation; (C) Cell elongation (length/ width) on different nanofibrous scaffolds after 24 hr of adhesion and proliferation ($p < 0.01$). n = 6.	31
Figure 5 Cell viability tests on nanofibrous membranes. (A) MTT assay of MSCs cultured on the membranes for 1, 4 and 7 days respectively. The cell viability has been normalized by setting the viability of the control on the first day as 100%. (B-F) Live/dead assay of MSCs cultured on TCPS as control (B) and nanofibrous membranes (C, G10P0; D, G7P3; E, G3P7 and F, G0P10) for 48 hr. Green and red represent for live and dead cells, respectively. Scale bars are 200 μm for all images.	35
Figure 6 Real time-qPCR of osteogenic gene expression levels of mouse MSCs cultured in vitro. Total RNA was prepared from MSCs grown on either induced, G0P0, G7P3, G3P7, G0P10	

groups for 1, 4 or 7 days. BSP(A), ALP(B), OC(C), OPN(D) gene expression was quantified using real time-qPCR methods, GAPDH was used as an internal control. Data values are expressed as mean \pm SE (n=3). “*” means p<0.05 vs the induced group. 38

Figure 7 Western blot analysis of p-ERK protein expression in mouse MSCs. Total protein was prepared from MSC grown on either induced, G0P0, G7P3, G3P7, G0P10 for one(A), four(B) or seven(C) days. β -actin was used as an internal control. Data values are expressed as mean \pm SE (n=3). “*” means p<0.05 vs the control group..... 40

Chapter I: Introduction

1.1 Background

There are multiple factors that regulate cells adhesion, migration, proliferation and differentiation in the microenvironment adjacent to the cells.[1-6] The microenvironment is composed of the extracellular matrix (ECM), the extracellular part of animal tissue that provides structural support and transfers nutrition and gas [7]. Many studies have developed synthetic ECM as matrices to mimic the native tissue structure to direct cell dynamic activities and further regulate specific tissue regeneration[8-16]. Over the years, the important role of the scaffolds in cellular processes has been broadly investigated. [17-20] For example, Brodbeck et al [21] investigated the effect of anionic and neutral hydrophilic scaffolds in raising the apoptosis in macrophage/ monocyte and decreasing macrophage fusion. However, most studies investigating the biomaterials to regulate cell fate have been focusing on the influence of mechanical properties of the scaffold [22-27]. Since cells interact with the scaffold on the cell-scaffold interface, the interfacial properties of the scaffolds such as the interfacial energy, hydrophilicity and surface topography also play a key role in directing stem cell fate [28].

Over the years, interfacial properties have been entailed to play increasingly important roles on a wide area of cellular functions ranging from cell dynamic activities [29-33] to the functionalities of biomolecules [34, 35]. It is now comprehended that direction on the cells through scaffold pathway may be carried out via multiple physical mechanisms, such as ECM topography and matrices elasticity and stiffness. In order to better understand and study cell behavior through better designed synthetic ECMs, both in physical ways and molecular interactions may help in engineering tissue substitutes from stem cells. Apart from physical

regulators, chemical properties of the scaffolds may also play an important role in controlling cell motilities. For example, it was found that integrin binding specificity can regulate the effects of surface chemistry on osteoblast differentiation and thus elicit desired cellular activities by engineering materials.[36] Nevertheless, up to now, the role of interfacial properties such as wettability independent of functional groups and mechanical properties on stem cell fate and differentiation has not been widely examined.

One of the challenges in understanding the effect of matrices interfacial properties has been simplifying its effects from those complex factors due to the bulk properties of the matrix. Here, we address the issue by designing tunable matrices in which the interfacial hydrophilicity/ hydrophobicity is regulated in a systematic manner by varying the mixing ratio of gelatin and polycaprolactone (PCL) electrospun nanofibrous membranes without altering the chemical functional group and mechanical properties of the matrix.

1.2 Hypothesis and objectives

In this project, I took advantage of a biomaterial design technique (electrospinning) to effectively produce a hydrophilic-hydrophobic composite environment to investigate the cell activities by tuning the wettability of the scaffold. The overall goal of the project was to regulate stem cell adhesion, motility and differentiation towards bone cells (osteogenesis) by varying the hydrophilicities of the composite electrospun nanofibres. Based on this goal, my hypothesis is that the interfacial hydrophilicity/hydrophobicity of the matrices, which determines how favorably (or unfavorably) the matrix interacts with the aqueous milieu, plays an important role in governing osteogenic differentiation of MSCs through ERK/12 pathway.

In order to realize this hypothesis, two objectives were set in steps: (1) to design and

fabricate a composite electrospun nanofibre with tunable wettability, low cytotoxicity and slow biodegradability and biocompatibility; (2) the mesenchymal stem cells (MSCs) differentiate towards osteogenesis based on different hydrophilicity through a specific pathway.

Chapter II: Literature Review

Mesenchymal stem cells derived from bone marrow (MSCs) are well known because of their ability to self-renew and produce certain phenotype of cell lines.[37, 38] Therefore, they are one of the most promising cell sources for the regeneration or repair of injured and diseased tissues. A lot of research has been concentrated on designing principles enlightened by basic mechanisms of cell-matrix interactions. However, despite the outstanding potential clinical future of MSCs, the application is currently held back by barriers that must be swept away.[39] These obstacles may appear discouraging, but nature has strategies to surmount them *in vivo*. The application is promising to ultimately extend our understanding of extrinsic regulators of cell fate; meanwhile latest techniques which are versatile enough are widely studied to summarize features of stem-cell microenvironments down to molecular scale. [6, 7, 40]

Therefore a major goal is to develop new methods, using better designed biomaterials, that more intimately mimic the native tissue structure and functions and thus promote differentiation of pluripotent cells without sacrificing the nature properties. *In vivo*, MSCs dwell within informative, tissue-specific surroundings that physically localize them and maintain their stem-cell phenotype.[41, 42] The major feature of stem-cell microenvironment is ability to keep stem cells slowly divided during homeostasis by balancing the percentage of motionless and activated cells. Stem cells will escape from the microenvironment if the tissue is injured and then proliferate dramatically, self-renew and differentiate to reconstruct the tissue.[43] In addition to being clear about the biochemical regulating functions of the stem cells, it is important to realize that the biophysical/mechanical features of the microenvironment, such as matrix mechanical properties and topographical cues are

extensively investigated to clarify the role of microenvironment elements around stem cells. [44]

Nowadays, though many clinical trials on animal models in which it has been qualified to inject stem cell engraftment *in vivo* are undergoing, only a few of the injected cells survived after several days or weeks. [45] Therefore to control stem cell migration, proliferation, and differentiation within complex *in vivo* surroundings is extremely challenging. As to the instinctive properties of plasticity and multilineage of stem cells are increasingly in need of regulating their growth, proliferation and differentiation. However, more evidence has indicated that a multiple series of extra environmental factors contribute to the overall control of stem cell motilities. In general, the regulation of stem cell fate has been attributed theoretically to genetic and molecular mediators such as growth factors and transcription factors. [46, 47] In particular, many fascinating studies showed an increasing cue on the vital feature of the native microenvironment such as the effect of ECM on stem cells with high attraction to the interactions between ECM ligands with receptors on the cell surface [48].

2.1 Cell-niche interactions and *in vitro* recapitulation

The niche refers to the *in vivo* microenvironment which has the ability to regulate stem cell self-renewal and differentiation. [49-51] There are three major components and interactions existing between cells and niche including growth factors, cell-cell interactions, and cell-matrix contacts. Growth factors added to culture or secreted by stem cells and their neighboring cells often play an important role in their effects on cell fate and embryonic development. Therefore growth factors are always strictly regulated in space and time. [52] It is necessary for viability that MSCs adhere to matrix or other cells because it is impossible

for individual cells to survive in suspension. Adhesive signals might be controlled as well as or better with artificial mimics. For example, in three-dimensional cultures, crosslinked hyaluronic acid (HA) hydrogels proved unique function in assisting ESC growth in undifferentiated masses which is possibly because that HA is a distinguished ECM natural polymer in embryonic development[53]. In culture, one way to control niche interactions in two dimensions is with topography of ECM prominency, which limits the modulating effects of matrix and cell contacts. Besides size control is also important to minimize gradients in physical or chemical factors such as oxygen that regulate stem cell fate [54]. The ECM not only influence cell adhesion and exhibits key cues to cells, but it also binds growth factors and thus limits their diffusion.

2.2 Biochemical cues regulate stem cell fate

Small molecules, regulating specific receptors in the signaling pathways, are emerging with distinct advantages for manipulating stem cell fates as valuable tools [55, 56]. These features allow temporal and flexible regulation of complex signaling interactions. Importantly, it is easy to control the effects of small molecules in a rapid and reversible way and they can be excellently mediated through changing concentrations and combinations of those small molecules. For example, regulating protein functions is much easier using small molecules than genetic management. Moreover, actually synthetic chemistry provide small molecules with theoretically unlimited potential for precisely controlling cell phenotypes for unlimited structure and functionality diversity, which could be widely studied by high-throughput screening based on phenotype [57-59].

Researchers have investigated several methods to automatically recognizing to screen in a molecular approach or combination of molecules that induce stem cell fate change [60-

62]. For example, arrays made from 192 specific combination groups of ECM and signaling molecules have been screened onto slides containing a thin coating of polydimethylsiloxane; and epithelial cadherin, placental cadherin, and JAG1 (a ligand for the receptor NOTCH1) were each found to promote the transferring of mammary progenitor cells into myoepithelial or luminal epithelial phenotypes [62]. The design of ECM molecules with biological related to stem-cell regulation is a critical approach towards defining the regulatory influences of the stem-cell microenvironment. Therefore biomaterials methods have been investigated to define the identity, concentration and patterns of soluble or ECM molecules singly and in combination. [63, 64]

Based on the knowledge of mechanisms of neural development and hESC differentiation, Chamber and his colleagues [65] developed an efficient neural differentiating protocol for hESCs that avoids the conventional embryoid body formation and found that combination of SB431542 (TGF β receptor inhibitor) and Noggin (a natural BMP antagonist) enhances rapid neural formation of more than 80% of hESCs in a monolayer manner. Those two signaling pathway inhibitors appear to react together to destabilize self-renewal of hESCs and prevent cells from differentiating into trophectoderm, mesoderm, and endoderm lineages. This study indicated that it can be achieved that directed ESC differentiated toward a specific lineage by deliberately combining the inductive signals for the desired cell lineage and the inhibitory signals blocking ESC self-renewal and their differentiation toward undesired lineages.

Chemical approaches have been particularly useful for accelerating differentiation process, increasing differentiation efficiency, and normalizing different differentiation propensity [66]. Chemical approaches could accelerate transferring of stem cell research into clinical application. First, chemical approaches could mediate stem cell fate and function *in vitro* using robust tools to precisely trigger safe, homogenous, and functional cells for cell

therapy in a sufficient number. Many issues in cell-based therapy even with transplantable cells, including immune-related ones, cell homing, engraftment, and long-term maintenance of transplanted cells' functions in the target tissue remains challenging. But to develop and manufacture cell-based therapy typically is more complicated and such therapy also more expensive for patients than conventional small-molecule and protein therapeutics. On the other side, chemical approaches also offer a supplementary method by directly modulating tissue-specific stem/progenitor cells *in vivo* for therapeutic purposes. [67-69]

2.3 Cell shape regulates stem cell fate

Among all the regulators of cell fate, cell shape is outstanding in cell growth and physiology [70] and related to many activities in embryonic development and stem cell differentiation. For example, changes in cell shape have been considered as a promising mechanism that controls myocardial development [71], while the growth and differentiation of capillary endothelial cells are partially regulated by ECM-caused changes in cell shape [72]. Many studies of the influence of cell shape on cellular differentiation are investigated along with the designation of three-dimensional culture networks, in which generally a more rounded, spheroidal cell morphology is induced compared to traditional two-dimensional culture systems. Extending this mechanism to stem cells, many researches have proved that stem cell fate can be influenced artificially by directing their shape using artificial ECM. For instance, when culturing chondrocytes on a flattened 2D surface, the cells become to “dedifferentiation” status and a shift from a chondrocytic phenotype to a more fibroblastic phenotype was observed [73]. However those cultured on a 3D system using pellet culture [46] or by encapsulation in a gel such as hyaluronic acid or alginate maintains their normal phenotype [74]. A number of researches have evidenced that it is necessary to possess a

rounded cell shape in order to obtain the differentiation of stem cells into a chondrocytic phenotype [2, 75, 76]. It is verified that a more rounded nuclear shape was relevant to the greatest expression of molecular markers corresponding to chondrogenesis with comparisons of cell and nuclear shape of MSCs [77]. Same as to murine embryonic stem cell-derived embryoid bodies maintained in 3D environment in poly (ethylene glycol) (PEG)-based hydrogels were also observed to be important up-regulation of cartilage-related markers compared to a 2D culture environment [78]. However when use the same medium and fibrin or gelatin as a matrix, which possesses similar mass properties but allow cell adhesion and a spread shape in 3D environment, results in a fibrochondrogenic phenotype [79].

Apart from physical control of shape, part of the effects may be caused by altered adhesive interactions between the cells and substrate, although many studies have controlled for such effects. The effects of cell shape on cellular signaling seem to extend well beyond its influence on adhesion signaling alone [5, 80]. The interactions between many external and internal factors that influence cell shape are varied and complicated and may involve relatively long-term interactions with the niche, as well as more acute changes because of physical factors such as mechanical or osmotic stress [29, 77, 81, 82].

The mechanisms behind of which cell shape regulates stem cell fate have been explored in fancy techniques that deposition of micropatterned proteins on a substrate, thus precisely governing the area of cell attachment. In artificial systems, the effect of a 3D cell morphology can be further modified by the presence of transforming growth factor beta 1 (TGF- β 1) [78] or interactions between cell surface receptors and ECM molecules [83]. Some studies have depicted a novel approach that the shape of MSCs can be dynamically modified in hydrogels created from photodegradable poly (ethylene glycol)-based scaffolds [84]. MSCs enclosed in a densely crosslinked gel exhibited a rounded morphology but could be elicited to a spread shape by reducing the crosslinking level of the gel via photodegradation,

so that controlled temporal changes could occur in the physical interactions between cells and hydrogels.

2.4 Biophysical cues regulate stem cell fate

Whether *in vitro* or *in vivo*, cells not only generate cellular force and are also often exposed to forces from either intrinsic or extrinsic environment. Both those forces can influence stem cell fate. Most researches have proved that surface mechanical properties could have significant influence on cell proliferation and especially differentiation. Early proof of the fact that ECM stiffness can influence cell differentiation was noticed in studies showing qualitatively that mouse mammary epithelial cells showed increased differentiation when grown on soft collagen gel substrates, as opposed to tissue culture plastic [85]. Mechanical deformations or strains are common in solid tissues such and imposing substrate strains of only 5% can cause MSCs differentiation toward smooth muscle [86]. Myogenic markers are upregulated when MSCs are cultured on hard scaffolds that mimic the elasticity of muscle and coated with collagen I, meanwhile when MSCs are cultured on hard gels that mimic precalcified bone, the cells show osteogenic differentiation [18]. Cells that attach to a matrix have been displayed to employ contractile forces, causing tensile stresses in the cytoskeleton[82]. Moreover, the relationship between these forces and the mechanical stiffness or elasticity, of the ECM can have a major influence on cell behaviors such as migration [3, 87], apoptosis [88] and proliferation [89]. Added induction factors can broaden or oppose this programming MSCs by matrix, whereas cell lines that are already committed to muscle or bone appear less responsive to the same cues. These later examples suggest not only physical attribute to differentiation but also carefully made materials can help prime the expansion of specific progenitors.

Cells grown on soft matrigel or on matrigel copolymerized with heat-denatured collagen exhibited reduced expression of actin and focal-adhesion plaque as compared to cells remaining in a monolayer pattern on rigid matrigel coat or on matrigel copolymerized with type I collagen [90]. In other cell phenotypes, myoblasts were grown on collagen strips attached to glass or polymer gels of differing mechanical stiffness. While the fusion of myoblasts into myotubes was found to be independent of substrate stiffness the development of actin/myosin striations occurred only on gels that had properties similar to those of normal muscle [91].

Most studies have been concentrating on the assumption that the mechanical properties of the native ECM have a significant influence on stem cell lineage specification. MSCs grown on multiple compliant polyacrylamide gel were found to have alterable properties related to the stiffness of the matrix, i.e. harder substrates induced cells with higher stiffness such as osteoblasts. Softer matrix (~100-500 Pa) enhanced neuronal differentiation, whereas stiffer matrix (~1,000-10,000 Pa) led to glial differentiation. Cell spreading, self-renewal, and differentiation were inhibited on soft matrix (10 Pa), whereas the cells grown on matrix with larger moduli more than 100Pa displaying upregulation of a neuronal marker, beta-tubulin III, on matrix that had the approximate stiffness of brain tissue. Moreover, the stiffness of the matrix governed the differentiation directions of the MSCs: soft substrates that mimic the mechanical properties of brain tissue were found to have neurogenic differentiation, substrates of intermediate stiffness that mimic muscle were myogenic differentiated, and relatively hard matrix with bone-like properties were found to be osteogenic differentiated [18]. Similarly, the effective stiffness of the underlying matrix has been observed to regulate the differentiation of NSCs [4].

There are other studies showing that MSCs could be retained quiescent by growing them on polyacrylamide substrates that mimicked the properties of marrow [92]. MSCs

seeded meagerly on the gels showing pending progression through the cell cycle and could be triggered to re-enter the cell cycle when presented with a stiff substrate. These cells could be induced into adipogenic or osteogenic pathways as well when grown in the proper induction medium suggesting that a soft substrate mimicking the bone marrow niche can retain MSCs in a quiescent state while preserving their multilineage potential. An important conclusion of this research lied on the fact that mechanical signals from the elasticity of the ECM may serve as a critical factor in the bone marrow niche that allows the maintenance of MSCs as a supplier for a long period [92].

Recent mechanical measurements of fibrotic scars that develop after an acute myocardial infarction [93] or with more chronic stimuli [94] show that the fibrotic tissue is locally rigidified by at least several-fold compared with normal tissue. Rigid fibrotic tissue can contribute a homing signal. In a gradient of elasticity, cells thereby accumulate on stiffer matrix in a process of durotaxis, which might constitute a biophysical basis for why MSCs home to sites of injury and fibrosis. *In vivo*, when stem cells export from their niche into the circulation [95] or when stem cells are injected intravenously as part of a therapeutic regimen, fluid forces push and pull the cells. Recent models of a scar-in-dish have indicated that the well-studied differentiation of fibroblasts to myofibroblasts requires both a stiff matrix (more than 20kPa) and TGF- β , with growth factor released from the ECM dependent on cell contraction-driven unfolding of the ECM complex that sequesters the TGF- β [96].

It should be noticed in these studies that multiple tissues could have similar elasticities, and therefore it may be hard or impossible to define unique stem cell differentiation by a single serie of mechanical properties. This further emphasizes the complexity of the interactions between intrinsic and extrinsic properties of stem cells and their niche in determining their fate [97].

2.5 Nano-biosystem interface regulate stem cell fate

At the interface of nanomaterials and biological systems, the organic and synthetic fields combine to a new science concerned with the safe use of nanotechnology and nanomaterial design for biological applications. The nano-bio interface comprises the dynamic physicochemical interactions, kinetics and thermodynamic exchanges between nanomaterial surfaces and the surfaces of biological components such as proteins, membranes, phospholipids, endocytic vesicles, organelles, DNA and biological fluids [98, 99]. Cells have the capability to discern micro- and even nanoscale geometric cues from their environment. Such cues may represent differences in molecular composition, surface topography or roughness, fibre diameter, or other parameters. Cell alignment is observed to be similarly influenced, from which the directional growth and differentiation of adult rat hippocampal progenitors cultured on micropatterned polystyrene substrates chemically modified with laminin exhibited over 75% alignment in the direction of the grooves, as well as significantly increased expression of neuronal markers [100]. These results indicated that the 3D topography of the matrix, together with matrix composition, can facilitate neuronal differentiation and neurite alignment. Furthermore, cells seem to be able to direct such architectural cues extends to nanoscale topographical features. MSCs seeded on nanoscale grooves of 350 nm width displayed alignment of their cytoskeleton and nuclei of MSCs along the grooves [101]. A significant up-regulation of neuronal markers such as microtubule-associated protein 2 was noticed on those substrates when compared to un-patterned and micropatterned controls. While the combination of such nanotopographic cues with biochemical cues such as retinoic acid further enhanced neurogenesis, nanotopography showed a stronger effect compared to retinoic acid alone on an un-patterned surface.

Previous studies have proved that the precise spacing between nanoscale adhesive

islands on a substrate can modulate the clustering of the associated integrins and the formation of focal adhesion and actin stress fibres and , in this way, control the adhesion and spreading of cells [102]. The mechanisms with which nanotopographic cues influence stem cell proliferation and differentiation are not well studied but appear to involve changes in cytoskeletal organization and structure, potentially in response to the geometry and size of the underlying features of the ECM. Changes in the feature size of the scaffold may influence the clustering of integrins and other cell adhesion molecules, thereby altering the number and distribution of focal adhesions. Gerecht et al. have used polydimethylsiloxane (PDMS) grating to induce the alignment and elongation of embryonic stem cells [103]. They also found that nanotopographic cues diversified the organization of various cytoskeletal components, including F-actin, vimentin, and α -tubulin, and the observed changes in proliferation and morphology were abolished by the effect of actin-disrupting agents. The nanotopographic features of the ECM have been shown to alter the morphology and proliferation of human embryonic stem cells through cytoskeletal-mediated mechanisms. Alternatively, the influence of nanotopographic features may be mediated through secondary effects, such as alterations in the effective stiffness perceived by the cell or differences in protein adsorption due to the structural features of the matrix.

The interface between nanomaterials and biological systems comprises a dynamic series of interactions between nanomaterial surfaces and biological nanoscale or nanostructured surfaces. These interactions are shaped by a numerous of forces that could ascertain whether the nanomaterial is bioavailable and may participate in biocompatible or bioadverse interactions. Investigating these various interfaces demands new ideas and imaging techniques. [104]

Chapter III: Materials and Methods

3.1 Materials

Polycaprolactone (PCL, Mw=80,000), gelatin (type A from porcine skin), 2, 2, 2-trifluoroethanol (TFE) and glutaraldehyde (GA, 25% in H₂O) were all obtained from Sigma-Aldrich. Dulbecco Modified Eagle's Medium (DMEM), fetal bovine serum (FBS), phosphate buffered saline (PBS) and trypsin-ethylenediaminetetraacetic acid (EDTA) were purchased from Gibco. Mouse bone marrow derived mesenchymal stem cells (MSCs) were purchased from the American Type Culture Collection (ATCC, USA).

3.2 Fabrication of electrospun nanofibrous membranes

The polymer solution with concentration of 6 wt% was prepared by dissolving PCL and gelatin with a weight ratio of 100:0 (PCL only) (G0P10), 70:30 (G3P7), 30:70 (G7P3) and 0:100 (gelatin only) (G10P0) in TFE and magnetically stirred for 24 hours at room temperature. The solutions were electrospun from a 22-gauge syringe with a needle diameter of 0.4 mm and mass flow rate of 1 ml/hr. A high voltage (12kV) from a high voltage power supply (Harvard Apparatus, BTX ECM600 Electroporation System) was applied to the tip of the needle attached to the syringe when a fluid jet is ejected. Polymer solution was ejected from the needle tip towards a plate collector which was covered with aluminum foil. The needle was located at a distance of 10cm from the ground collector. All membranes were obtained after 8-12 hr of fibre deposition. The fibrous membranes were cut and shaped into 6 mm in diameter.

The thickness of the gelatin/PCL nanofibrous membranes was measured with the aid of a micrometer (Mitutoyo, Japan) and their apparent density and porosity were estimated through the following equations [105]:

Gelatin/PCL nanofibrous membrane apparent density (g cm^{-3})

$$= \frac{\text{Mass of membrane (g)}}{\text{Membrane thickness (cm)} \times \text{Membrane area (cm}^2\text{)}} \quad (1)$$

Gelatin/PCL nanofibrous membrane porosity (%):

$$= \left(1 - \frac{\text{Membrane apparent density (g cm}^{-3}\text{)}}{\text{Bulk density of gelatin/PCL (g cm}^{-3}\text{)}}\right) \times 100\% \quad (2)$$

The electrospun gelatin/PCL nanofibres were crosslinked by exposure to the vapor of glutaraldehyde in dark drawer for 24 hr at room temperature. The crosslinked nanofibres were then repeatedly washed with double-distilled water and air dried at room temperature.

3.3 Characterization of nanofibres

3.3.1 Contact angle measurement

The water contact angles of the nanofibrous membranes were determined by a sessile drop method at room temperature (20°C) using contact angle meter (CAM100, KSV Instruments Ltd.). A 4 μl droplet of deionized water was dropped onto the flat surface of fibrous membranes. The contact angles which are the angles measured through water drop, where the water/air interface meets the solid scaffolds, indicating the wetting ability of the membranes were measured automatically. All samples were prepared in triplicate and the results were shown as a mean value \pm standard deviation.

3.3.2 IR-ATR spectroscopic analyses

Chemical analysis of the nanofibrous membranes (all four groups, i.e. G10P0, G7P3, G3P7 and G0P10) before crosslinking were carried out by Infrared attenuated total reflectance (IR-ATR) spectroscopy (Avatar 380, Thermo Nicolet, Waltham, MA, USA) over a range between 4000 and 400 cm^{-1} at 2 cm^{-1} resolution averaging 100 scans.

3.3.3 *In vitro* degradation

The nanofibrous scaffolds were cut into 1 × 1 cm in size for in vitro degradation testing. The membranes were weighed and then kept in phosphate-buffered saline (PBS, 0.1M, pH 7.6) and Dulbecco modified Eagle's medium (DMEM) respectively and incubated at 37°C. At specified time intervals, the membranes were taken out from the solution, washed with distilled water, dried, and weighed. The degree of in vitro degradation was indicated as the following:

$$\text{Membrane degradation (\%)} = \frac{\text{weight difference (i.e. before-after soakage)}}{\text{weight before soakage}} \times 100\%$$

3.3.4 XPS characterization

XPS experiments were taken on a PHI-5000C ESCA system (Perkin Elmer) with Al K α radiation. The X-ray anode was run at 250 w and the high voltage was remained at 14.0 kV with a detective angle of 54°. The pass energy was set at 92.4 eV to ensure sufficient sensitivity. The base pressure of the analyzer chamber was about 5 × 10⁻⁸ Pa. Both the total and narrow spectra of all the elements with a very high resolution were measured. Binding energies were calibrated by using the containment carbon (C1s = 285.1eV).

3.4 Cell culture

Biological assays were performed using MSCs. Firstly, the cells were plated as a monolayer and cultured to confluence in DMEM containing 10% FBS and 1% penicillin (100 units ml⁻¹) (Sigma). Medium was replaced every three days and the culture was maintained in a humidified incubator at 37°C with 5% CO₂. Once the cells reached 80% confluence, they were trypsinized and passaged to the next generation.

The nanofibrous scaffolds were exposed to UV for 30min, washed with ethanol for 15min and with PBS for 5 min triple times. After reaching 80% confluence, the cells were detached by trypsin-EDTA and viable cells were counted by trypan blue assay. Cells are further seeded onto nanofibrous scaffolds, placed in Petri dishes at a seeding density of 5×10^4 cells/sample and cultured in medium at 37C and 5% CO₂ for certain time before harvest.

3.5 Scanning Electron Microscopy (SEM) for substrate and cell morphological examination

The morphology of nanofibrous scaffolds and cells after 24hr seeding were processed for scanning electron microscopy (SEM) (SEM, Cambridge Stereoscan 120) at an accelerating voltage of 10 kV. Briefly, the substrates cultured with MSCs were washed with PBS (0.1M, pH 7.4) solution three times and then fixed in 4% paraformaldehyde solution for 1 hr. After fixation, they were washed 3 times with distilled water for 10 min each wash. Then the samples were dehydrated through a series of graded ethanol solutions (50, 70, 90 and 100%) for 30 min each and left in 100% ethanol. Next, the samples were mounted onto stubs and sputter coated with gold using a Denton Desk II sputtering before scanning by SEM.

Cell elongation measurements were processed using ImageJ software following the

formula:

$$\text{Cell Elongation (\%)} = \frac{\text{average cell length}}{\text{average cell width}} \times 100\%$$

3.6 Cell viability study

To study cell proliferation on the substrates, viable cells were determined by using colorimetric MTT assay (CellTiter 96[®] Aqueous Assay, Madison, WI, USA). The mechanism behind the MTT assay is that metabolically active cells will react with the tetrazlium salt in the MTT reagent to produce a soluble formazan dye that can be absorbed at 570nm. After 2 days of cell seeding in a 96-well plate with the nanofibres, the substrates were rinsed with PBS, followed by incubation with 20% MTT reagent in serum-free culture medium for 3 hr. Thereafter, aliquots were pipetted into the 96-well pate. The 96-well plate was then placed into a spectrophotometric plate reader (FLUOstar OPTIMA, BMG Lab Technologies, Germany) and the absorbance at 570nm and 630nm of the content of each well was measured.

Cell viability was also tested using Live/Dead assay according to the protocol provided by InVitrogen Canada Inc. Prior to cell culture, the bottom of the culture dish was coated with a layer of agarose gel to prevent cell adhesion. For staining, cells at a concentration of 50,000cells/ml were cultured with the nanofibrous membranes for 2 days and then incubated in cell culture medium containing 2 μ M calcein AM and 4 μ M ethidium homodimer probes for 20 min. Then the membranes with cells were rinsed with PBS, dried and mounted onto slides. Images were taken under a confocal laser scanning microscopy (Olympus FV1000, Japan).

3.7 Real-Time PCR

3.7.1 Cell lines and treatment

5×10^4 MSCs were seeded onto the nanofibrous membranes and allowed to settle for 2 hrs. Then, 2 ml medium was added to the disk. After 3 days cultivation, cell-membranes were transferred to FBS-supplemented DMEM containing a combination of osteogenic chemical supplements: 50 µg/ml L-ascorbic acid 1-phosphate (Sigma), 10 mM β -glycerophosphate (Sigma) and 100 nM dexamethasone (Sigma). Membranes with cells were returned to the incubator for 1, 4 and 7 days respectively. The osteogenic medium was changed for every 2-3 days.

3.7.2 Quantitative Real-time PCR analysis

At predetermined time intervals, the medium was aspirated with the unattached cells and the wells were washed with DPBS. Then, cells on the membranes were treated by liquid nitrogen and smashed. In order to validate the gene expression of osteogenic differentiation in all samples, total RNA isolation and cDNA synthesis were done by using TRIzol and Oligo dT (Invitrogen, USA), according to the standard procedures. Then quantitative Real-time PCR (qPCR) was performed by SYBER Green assays (Applied Biosystems, USA). Amplification conditions were as follows: Hold in 95°C for 10 minutes, followed by 40 cycles of 15 seconds at 95°C and 1 minute at 60°C. Thermal cycling and fluorescence detection were done using the StepOnePlus™ Real-Time PCR System (Applied Biosystems, USA). The mRNA expression levels were determined relative to the GAPDH by the $\Delta\Delta C_t$ method. Primer sequences were synthesized as shown in Table 1.

Table 1 Sequences of primers for the qRT-PCR

Gene	Forward primer sequence	Reverse primer sequence
BSP	5'-ccacactttccacactctcg-3'	5'-cgtcgcttccttcacttttg-3'
ALP	5'-ctccaaaagctcaacaccaatg-3'	5'-atttgtccatctccagccg-3'
OC	5'-acactctaaagggttgac-3'	5'-tcccatgctgtgaccctctagagg-3'
OPN	5'-ctacgaccatgagattggcag-3'	5'-catgtggctataggatctggg-3'
GAPDH	5'-aggtcggtgtgaacggatttg-3'	5'-tgtagaccatgtagtgagggtca-3'

OC osteocalcin, BSP bone sialoprotein, OPN osteopontin, ALP alkaline phosphatase, GAPDH glyceraldehyde-3-phosphate dehydrogenase.

3.7.3 Western Blot Analysis

At the predetermined time intervals, the medium were aspirated with the unattached cells and the wells were washed with DPBS. Then, cells on membranes were treated by liquid nitrogen and smashed. Whole proteins were isolated by RIPA buffer (50 mmol/L Tris-HCl, pH 8.0, 150 mmol/L NaCl, 0.1% SDS, 1% NP-40, 0.25% Sodium deoxy-cholate and 1 mmol/L EDTA) with a freshly added protease inhibitor cocktail (Roche). Total protein concentrations were determined by BCA Protein Assay (KeyGEN). Proteins (20 µg/lane) were separated on 12% SDS-PAGE and electrophoretically transferred to PVDF membranes. The membranes were blocked for 2 h at room temperature in TBS-T buffer (10 mmol/L Tris-HCl, pH 7.5, 500 mmol/L NaCl, 0.05% Tween 20), containing 5%(w/v) skim milk, and incubated antibodies against ERK1/2 and phosphor-ERK1/2(Bioworld) at 4°C overnight. After incubation with the primary antibody, the membranes were washed three times with TBS buffer and incubated with the appropriate HRP-linked secondary antibodies for 1 h at room temperature. The optical density was determined using the Supersignal

Chemiluminescent substrate (Santa Cruz) according to the manufacturer's instructions.

House-keeping gene β -actin was used as an internal standard.

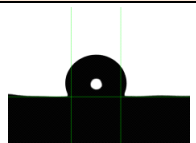
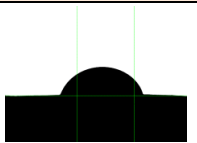
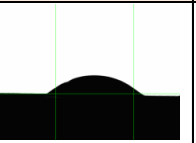

3.8 Statistical analysis

All data presented are expressed as mean \pm standard deviation (SD). Statistical analysis was carried out using single-factor analysis of variance (ANOVA). A value of $p \leq 0.05$ was considered statistically significant.

Chapter IV: Results and Discussion

4.1 Design of tunable matrices with varying wettability

Table 2 Contact angle measurement of gelatin/PCL (G/P) nanofibres.

G/P	G0P10	G3P7	G7P3	G10P0
Average contact angle (°)	117.85 \pm 4.15	55.78 \pm 1.65	29.27 \pm 2.77	0
Initial images of waterdrops on the membranes				

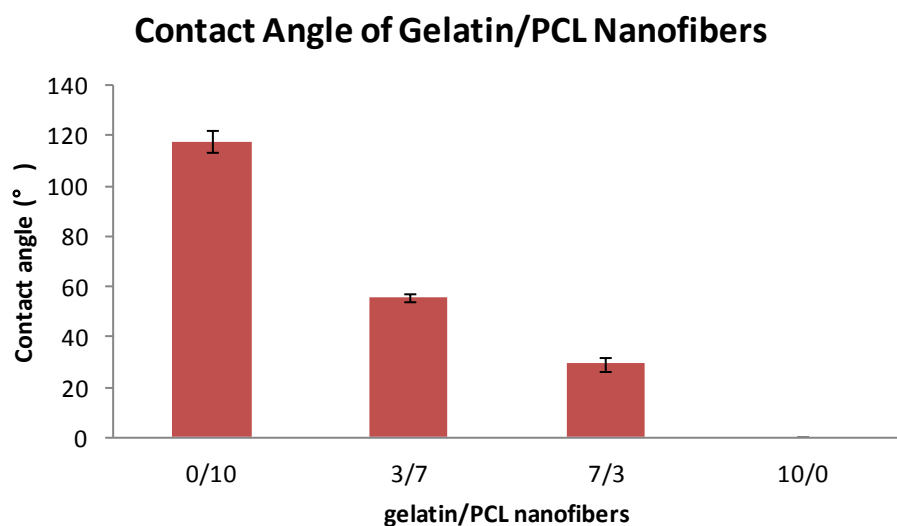


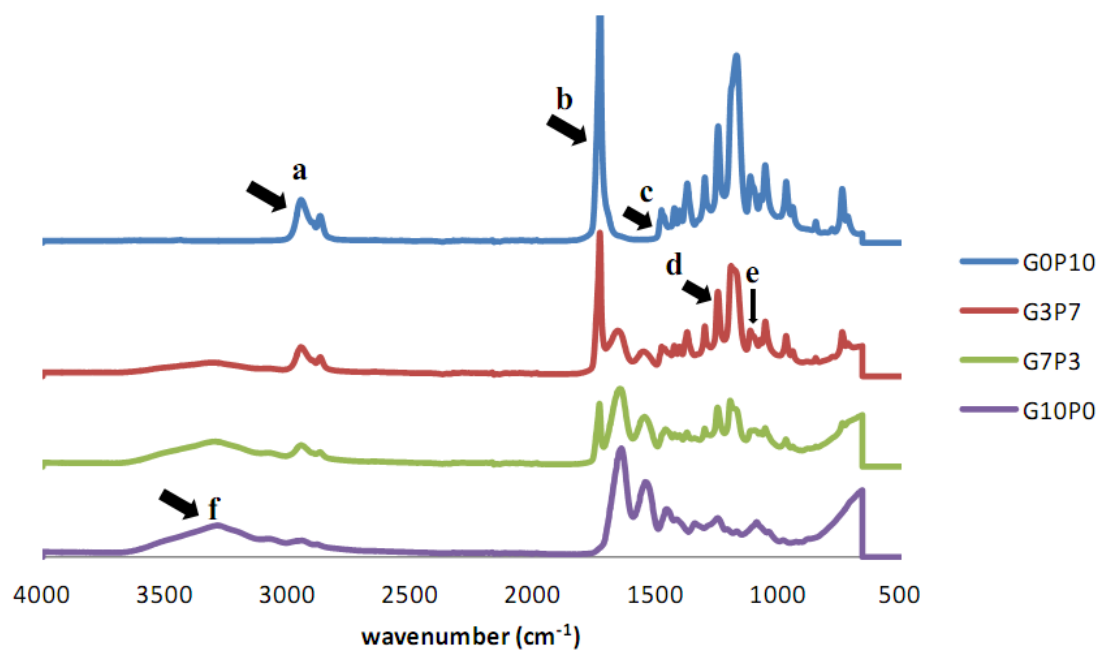
Figure 1 Contact angles of different electrospun fibrous membranes. From pure PCL (most left column) to pure gelatin (most right column) the membranes show a significant decrease in water contact angle, indicating a gradual decreasing trend in wettability.

Electrospinning is a simple and versatile technique for producing fibres with diameters in the sub-micrometer or even nanometer range. [106, 107] A vast array of materials such as polymers, ceramics and their composites can be manufactured into ultrathin fibril structures

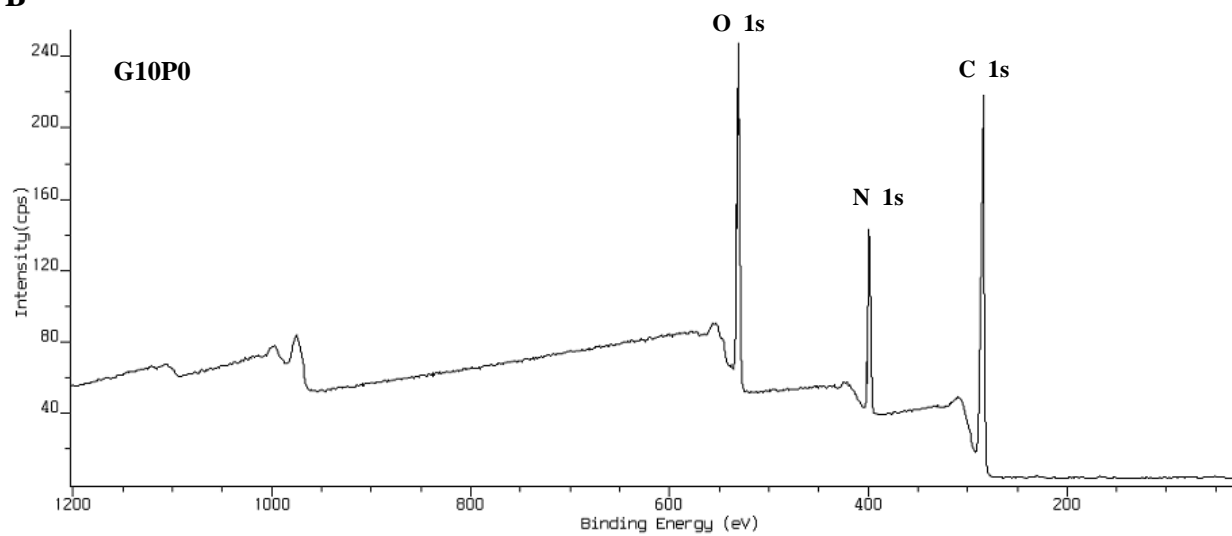
using electrospinning method. It is well known that cells interact strongly with their environment (ECM). This structure, which is primarily composed of collagens, exhibits varying fibre diameters that are quite frequently one or more orders of magnitude smaller than the cell itself. Electrospinning allows the production of these small fibre diameters in sub-micron dimensions, down to about 50nm. [108-112] Gelatin is a natural protein with high hydrophilicity while PCL is highly hydrophobic. These two compounds have been widely used to fabricate electrospun nanofibres as biomaterials due to their excellent biocompatibility. Here, we have fabricated tunable composite electrospun nanofibrous matrices with precise control over their hydrophobicity by mixing gelatin and PCL in different ratios, ranging from 0/10 to 10/0 gelatin/PCL ratios. These matrices are labeled G0P10, G3P7, G7P3 and G10P0 respectively depending on the gelatin/PCL ratios. The reduction in contact angle measurement from $(117.85 \pm 4.15)^\circ$ of G0P10 (100% PCL) to 0° of G10P0 (100% gelatin) shows that the hydrophilicity of the combination materials is reduced along with different mixing ratios of gelatin and PCL (Figure 1). With 100% gelatin in the composite scaffold, water drops are absorbed extremely fast by the matrices so that its contact angle is defined as 0° . On the contrast, on the PCL matrice, water hardly spreads on the surface showing an obtuse contact angle. This confirms the varying wettability of the surfaces of the nanofibrous scaffolds, and that the hydrophilicity of the scaffolds increased with increasing gelatin concentration. Either the hydrophobic or the hydrophilic surfaces are suitable for cell adhesion to vastly different extents.

4.2 Characterization of composite nanofibres

A



B



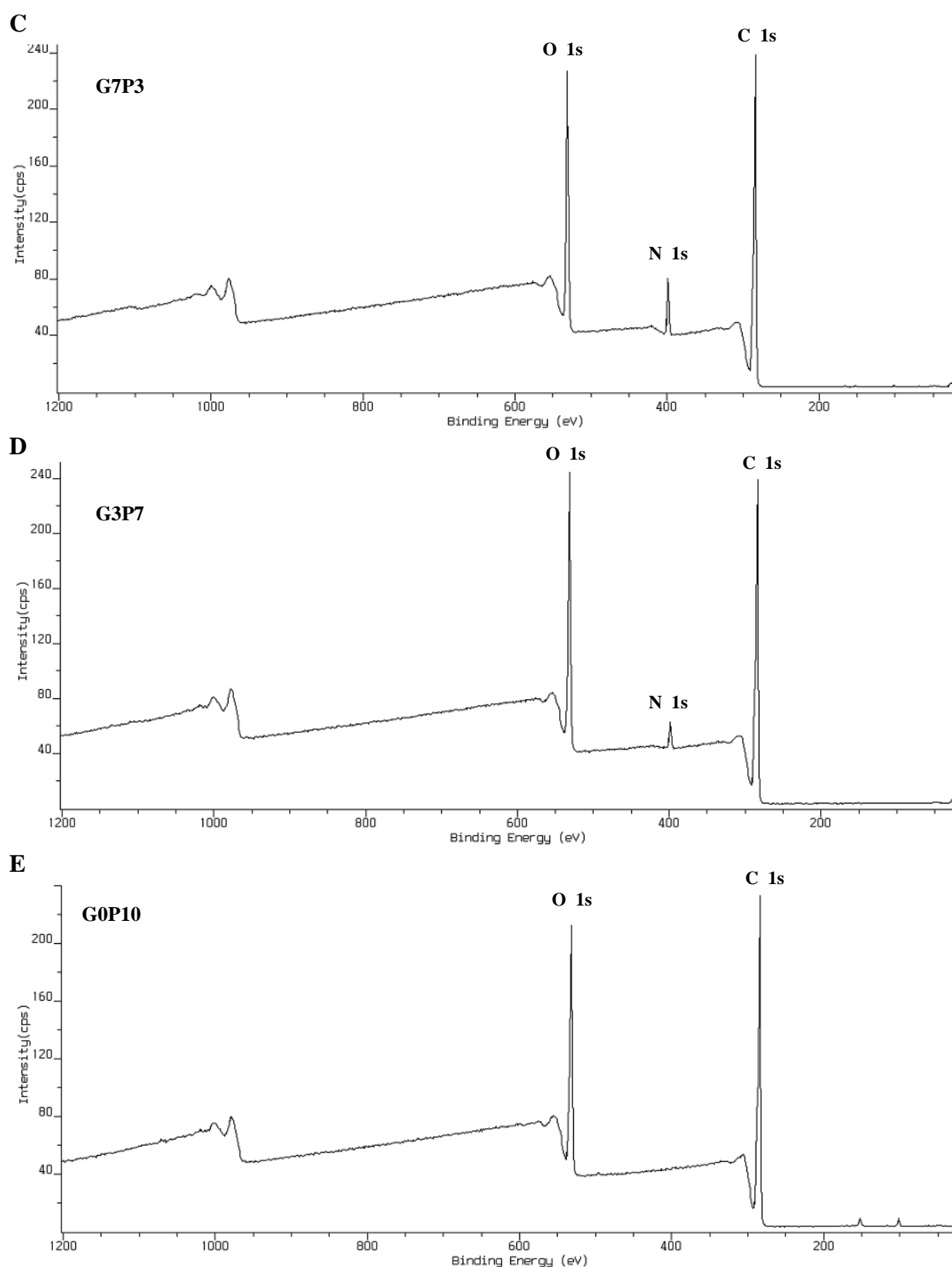


Figure 2 Characterization of nanofibres. (A) IR-ATR spectroscopic analysis of non-crosslinked gelatin/PCL nanofibrous membranes. (B-E) XPS analysis of nanofibres without

crosslinking. (B, G10P0; C, G7P3; D, G3P7; E, G0P10)

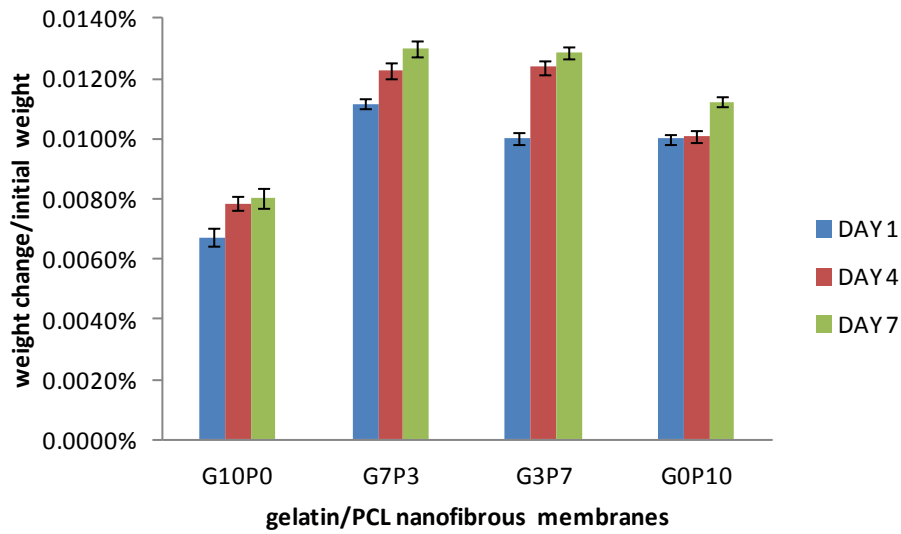
To confirm that the gelatin and PCL are mixed in specific ratios via electrospinning, IR-ATR analysis was carried out. IR-ATR is a testing technique used together with infrared spectroscopy which allows samples to be characterized directly on the solid surface without further preparation. Since all the cells grown, proliferation and differentiation occur on the surface of the nanofibrous membranes, the surface chemical structures of the samples were characterized instead of the mass characterization using Fourier transform infrared spectroscopy (FT-IR). Figure 2A shows IR-ATR spectra of the four groups of gelatin/PCL nanofibrous membranes before crosslinking. The peaks at 2944 and 2866 cm^{-1} in G0P10, G3P7 and G7P3 (Figure 2A-a) show a disappearing trend corresponding to the characteristic absorption of the C-H stretching bonds of $-\text{CH}_2\text{CH}_2-$, which are similar to those of ϵ -CL on PCL. Besides, the strong peak at 1723 cm^{-1} is due to the C=O absorption (Figure 2A-b). Similarly, a weak peak at 1470 cm^{-1} may be due to $-\text{CH}_2$ bending vibration (Figure 2A-c). Moreover, the peaks at 1240 and 1107 cm^{-1} are assigned to the characteristic C-O-C stretching vibration of repeated $-\text{OCH}_2\text{CH}_2-$ units of PCL and the $-\text{COO}-$ bond-stretching vibrations (Figure 2A-d and e). Additionally, typical bands are found such as N-H stretching at 3300 cm^{-1} for amide-A (Figure 2A-f), C-H stretching at 3068 cm^{-1} for amide-B, C=O stretching at 1651 cm^{-1} for amide-I, N-H deformation at 1544 cm^{-1} for amide II and N-H deformation at 1293 cm^{-1} for amide III.

X-ray photoelectron spectroscopy (XPS) analysis was carried on to study the surface chemistry of the nanofibrous membranes. The spectra of all four groups as shown in Figure 2B-E identified the elements of C, N and O. Though there's no significant difference between the peaks of C 1s and O 1s which is due to the similar C-O ratio in the chemistry structures of gelatin and PCL, the peaks of N 1s in different nanofibrous membranes

displayed an obvious change along with the change of gelatin-PCL ratio. The G10P0, G7P3 and G3P7 spectra all possessed an N 1s peak at 400 eV and the value of the peaks showed a decrease trend, indicating the reducing portion of gelatin in the composite. The atomic and mass concentrations of N 1s in G10P0 (pure gelatin) are 14.48% and 15.64% respectively, while in G3P7 are only 2.74% and 2.97% respectively. As shown in Figure 2E, the peak of N 1s disappeared indicating the lack of gelatin in G0P10 nanofibrous membrane. The XPS results confirmed the conformation of the nanofibrous membranes and quantified the gelatin-PCL ingredients.

4.3 In vitro degradation tests of the nanofibrous membranes

A



B

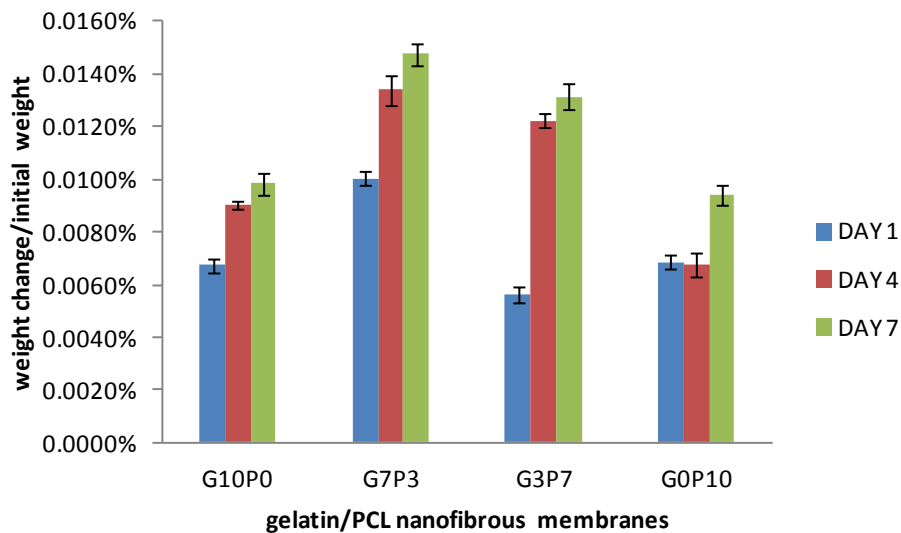


Figure 3 Degradation tests of gelatin/PCL nanofibrous membranes in (A) PBS and (B) cell culture medium for 1, 4 and 7 days. Bars indicate the mean values for all measured nanofibrous membranes, n = 5.

Gelatin, as a protein produced by the partial hydrolysis of collagen extracted from skin, bone, cartilage, ligaments [113], possesses high hydrophilicity and solubility in most aqueous solutions including phosphate buffered saline (PBS) and cell culture medium. Once placed in

the solutions, the pure gelatin or gelatin/PCL composite nanofibres dissolve immediately. To avoid this, glutaraldehyde (GA), an amine-reactive homobifunctional crosslinker, was used to confer the structural integrity of gelatin [114, 115]. The GA-crosslinked gelatin and gelatin/PCL composite nanofibrous membranes were soaked in PBS and cell culture medium (Dulbecco Modified Eagle's Medium, DMEM) for 1, 4 and 7 days respectively to evaluate the degradation degree *in vitro*. The nanofibrous membranes with different gelatin and PCL ratios were cut into square pieces ($1 \times 1 \text{ cm}^2$) and weighed before and after the specific degradation time. The degradation was showed in Figure 3. The extent of degradation of the nanofibrous membranes was slightly greater for the first 24 hours compared to the next 7 days. In both solutions, either PBS or DMEM, the weight change ratio of the membranes possessed a low value down to 0.006% (G3P7 on day 1) and the highest value of only 0.015% (G7P3 on day 7). The low order of magnitude of the weight change ratio indicated that from the physical point of view, the gelatin/PCL nanofibrous membranes barely dissolved or were absorbed by either PBS buffer or cell culture medium, which can be deemed as a guarantee of safely applying the nanofibrous membranes to further short-term cell cultivation and osteogenesis differentiation tests without concern about the effect due to scaffold degradation.

4.4 Matrices hydrophobicity-mediated cell adhesion and proliferation of MSCs

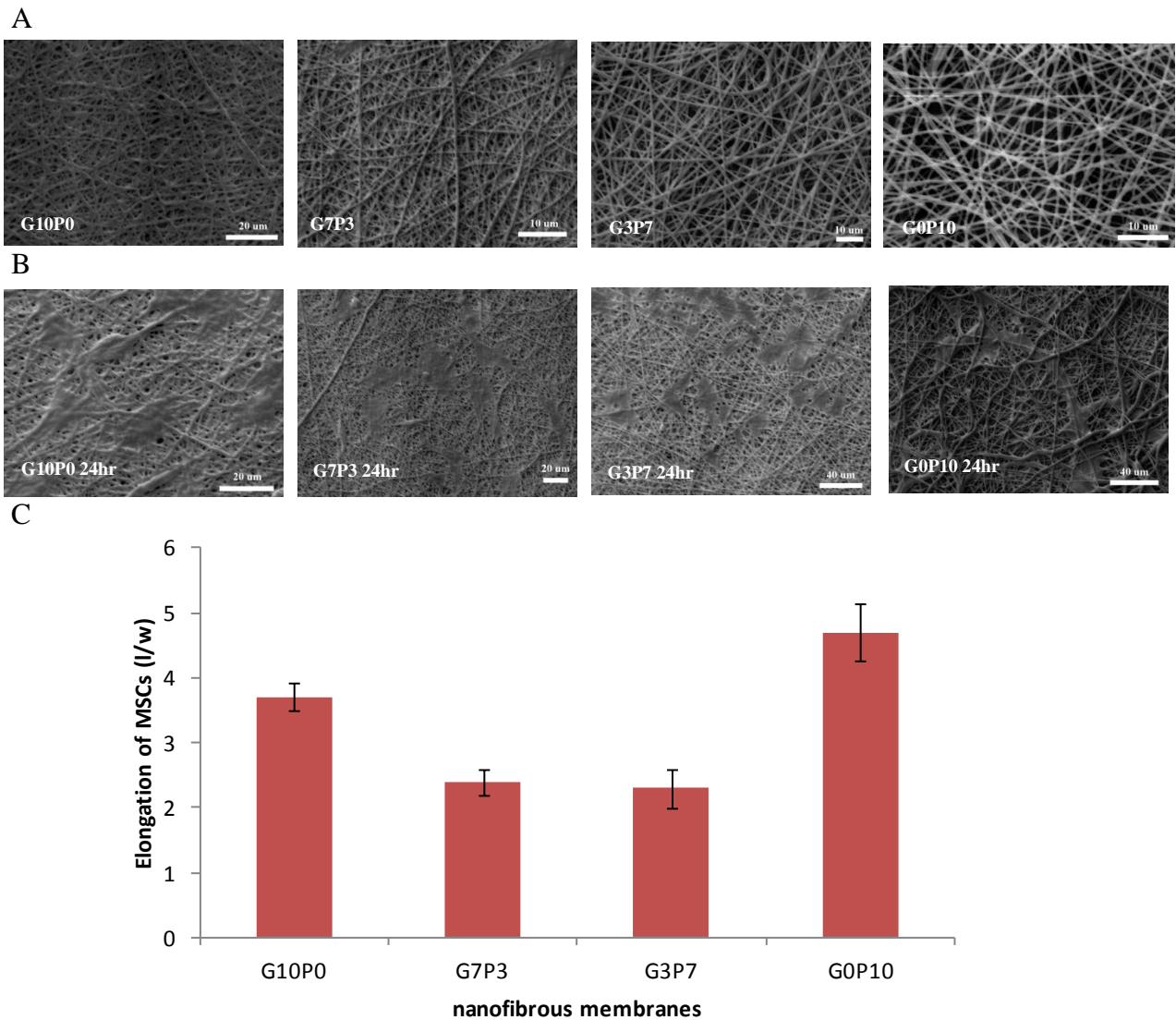


Figure 4 SEM micrographs of (A) gelatin (G10P0), gelatin/PCL (G7P3, G3P7) and PCL (G0P10) nanofibrous scaffolds (left to right); (B) MSCs on different nanofibrous scaffolds after 24hr of cultivation; (C) Cell elongation (length/ width) on different nanofibrous scaffolds after 24 hr of adhesion and proliferation ($p < 0.01$). $n = 6$.

Morphological images of the gelatin/PCL nanofibrous membranes were taken using SEM and are shown in Figure 4A. The micrograph image depicts randomly interconnected

structures and the seemingly smooth morphology of the electrospun gelatin/PCL nanofibre. The diameter of the nanofibre was estimated to be in the range of 400-900 nm (90% nanofibres), with a mean diameter of 780 ± 120 nm, by using image analysis software (ImageJ, National Institutes of Health, Bethesda, MD). The gelatin/PCL nanofibre mat with a thickness of around 30 μm was obtained through 2 hr of electrospinning. Porosity is deemed as a vital parameter for tissue engineering scaffolds. Such nanofibrous membranes which would be used for osteogenesis differentiation should largely be made porous. The porous nature of the scaffolds would then be beneficial for cellular infiltration and proliferation. On the other hand, the porous structure should continue to ensuring sufficient gas and nutrient exchange for viable tissue regeneration.

The preferred porosity of scaffolds used for cellular penetration should generally be within the range of 60-90% [116]. This could easily be achieved by using phase separation and solid free-form fabrication techniques. The porosity of the electrospun gelatin/PCL nanofibrous membranes in this study was estimated to be around 60-70%, comparable to the techniques formerly mentioned. The pores generated within the scaffold structure for cellular in-growth are formed by nanofibres touching and bonding to each other which are different from isotropic pores made by using particles or bubbles when the scaffold is solidified. Previous studies on gelatin/PCL nanofibres have also shown that the gelatin component of the co-polymer is gradually dissolved during cell culture, thus creating more spaces for cell migration. Similarly, the good elongation and deformation properties of gelatin allow easier opening of spaces for cell penetration to a deeper level of the membranes [117].

It is not easy to create well-defined pore sizes through the electrospinning technique because of the randomly deposited fibres. However, the overall network architecture structure mimics the natural ECM, and this provides an advantage in its application as a tissue engineering scaffold.

The cell morphology of the gelatin/PCL membranes was also studied by SEM after 24 hr of culture and the results are shown in Figure 4B. The composite nanofibres showed improved biological properties in terms of MSCs response compared to 100% PCL nanofibres. Nevertheless, the electrospun gelatin/PCL scaffolds showed good MSCs compatibility. Visually there were a relatively larger number of cells on the gelatin/ PCL scaffolds compared to that of the pure PCL scaffold. The MSCs spread and stretched themselves rather than contracting into a compressed and round shape as exhibited by the cells growing on the 100% PCL alone membrane (Figure 4B). To facilitate cell attachment onto the scaffolds, quite often one uses surface modification techniques via chemical and plasma treatment of biodegradable scaffold materials. For example, simply soaking scaffolds in a purified collagen solution before cell seeding makes use of the cells' favorable affinity to adhere to natural collagen. The disadvantage of this approach is that the collagen biomacromolecules are only coated on the surface of the fibrous scaffolds. Furthermore, it is achieved with a costly collagen material. At this point, current electrospun gelatin/PCL fibrous scaffolds provide an alternative solution to improve the biocompatibility of biomaterial scaffolds with tissues.

The composite scaffolds of gelatin/PCL nanofibrous membranes could allow cellular penetration or infiltration into the inside of the gelatin/PCL composite fibrous structure instead of just attaching onto the surfaces as exhibited on the PCL scaffold alone. This infiltration indicated a 3D cell growth. As shown in Figure 4B, more MSCs proliferated on the gelatin/PCL scaffold. The cells spread actively on the gelatin/PCL nanofibrous membranes and penetrate inside the scaffolds instead of just attaching to the surface as exhibited by the PCL nanofibrous scaffolds. With more gelatin ratio in the nanofibrous scaffolds, better hydrophilicity and cellular affinity obtained with consistent release of gelatin protein molecule from the composite nanofibrous scaffolds. The cell adhesion and proliferation were

also increased due to the increase of wettability of the scaffolds. Zhang et al. studied gelatin/PCL nanofibrous scaffolds and found that gelatin can be continuously released (leached out) over a time scale of more than 2 weeks in PBS solution at 37°C. The leaching kinetics can be governed by a progressive dissolution and diffuse mass transfer similar to that of an erosion process. These bicomposite porous nanofibres gradually caused the water-soluble gelatin to leach out from gelatin/PCL fibres [118].

To better understand the relationship between wettability and MSCs morphology, we undertook a quantitative analysis of cellular morphological shape. As shown in Figure 4C, the elongation ratio of MSCs increased with increasing content of gelatin in the composite nanofibrous membranes. Due to the similar surface chemical and physical properties, the MSCs on the nanofibrous scaffolds displayed a similar average elongation ratio of length/width range from 2.1 to 2.7. Nevertheless, these cell elongation results were also confirmed with cell morphology imaging by SEM, which is shown in Figure 4B. The micrographs show that a greater degree of elongation is evident among the MSCs cultured on gelatin and PCL nanofibrous scaffolds. This demonstrates that cell elongation and adhesion appear to be closely connected to surface hydrophilicity. The elongation of the MSCs on the nanofibrous scaffolds with more gelatin resulted in a preferential differentiation into osteogenic lineage, which was further confirmed by gene expression experiments introduced in the following sections.

4.5 Cell viability on nanofibrous membranes

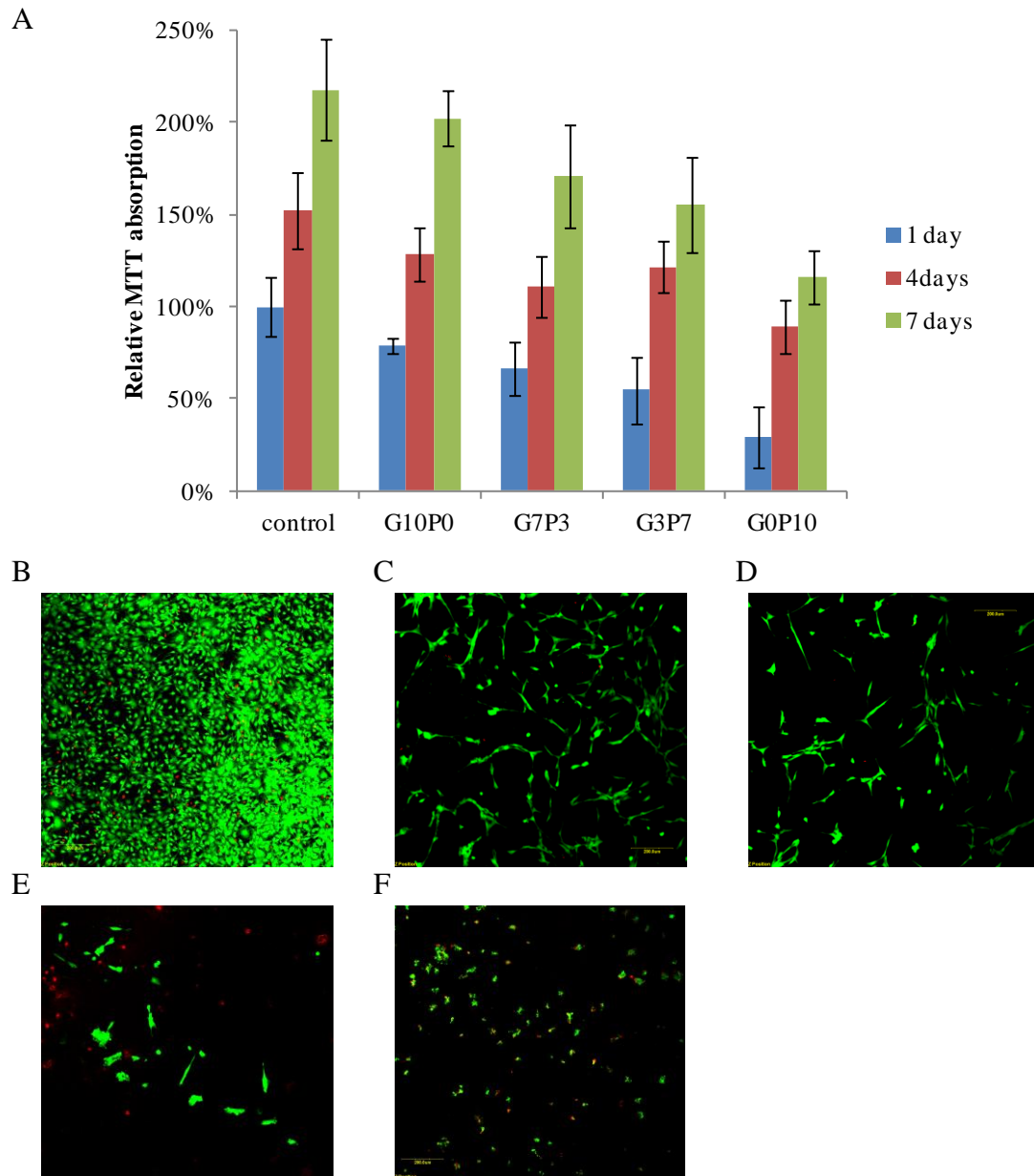


Figure 5 Cell viability tests on nanofibrous membranes. (A) MTT assay of MSCs cultured on the membranes for 1, 4 and 7 days respectively. The cell viability has been normalized by setting the viability of the control on the first day as 100%. (B-F) Live/dead assay of MSCs cultured on TCPS as control (B) and nanofibrous membranes (C, G10P0; D, G7P3; E, G3P7 and F, G0P10) for 48 hr. Green and red represent for live and dead cells, respectively. Scale

bars are 200 μm for all images.

The MSCs viability on nanofibrous membranes was assessed using the MTT assay after 1, 4 and 7 days (Figure 5A). The results indicate that on more hydrophilic matrices such as G10P0 and G7P3, cells possessed similar viability as on the control culture dishes. However, cell viability was significantly reduced on relatively hydrophobic matrices (G3P7 and G0P10) from $(54 \pm 10) \%$ to $(29 \pm 10) \%$ on the first day. The viability of cells cultured with hydrophobic matrices remained relatively low compared to those cultured on hydrophilic matrices in the next 3-6 days. The viability of cells on nanofibrous membranes was also qualitatively assessed using the Live/Dead assay (Figure 5B-F). In corresponding to the results of MTT assay, cells on hydrophilic matrices possessed a relatively higher viability than those on hydrophobic matrices, as well as a healthier morphology and significantly higher proliferation. These results suggest that increased hydrophilicity of the matrices could promote cell proliferation and viability in a significant manner.

4.6 Changes in mRNA expression of MSCs in bone-derived scaffolds made from different nano-membranes

To investigate whether different nano-membranes affected MSCs osteogenic differentiation, genes associated with osteogenesis, including BSP, ALP, OPN and OC, were measured by real-time RT-PCR on day 1, 4 and 7. G10P0 -stimulated BSP, ALP, OPN and elevated OC mRNA expression was apparent on the 1st day (Figure 6), and the elevated level of osteogenesis mRNA lasted for 3 days (Figure 6). However, osteogenesis expression for the G10P0 group showed a decreased level on day 7(Figure 6). On the contrary, the G0P10 group showed a marked accumulation on day 4 which lasted until day 7(Figure 6). In general, the trend from G10P0 to G0P10 revealed a decreased trend in osteogenesis expression on day 1 and the trend from G10P0 to G0P10 showed an increased trend in osteogenesis expression on day 7.

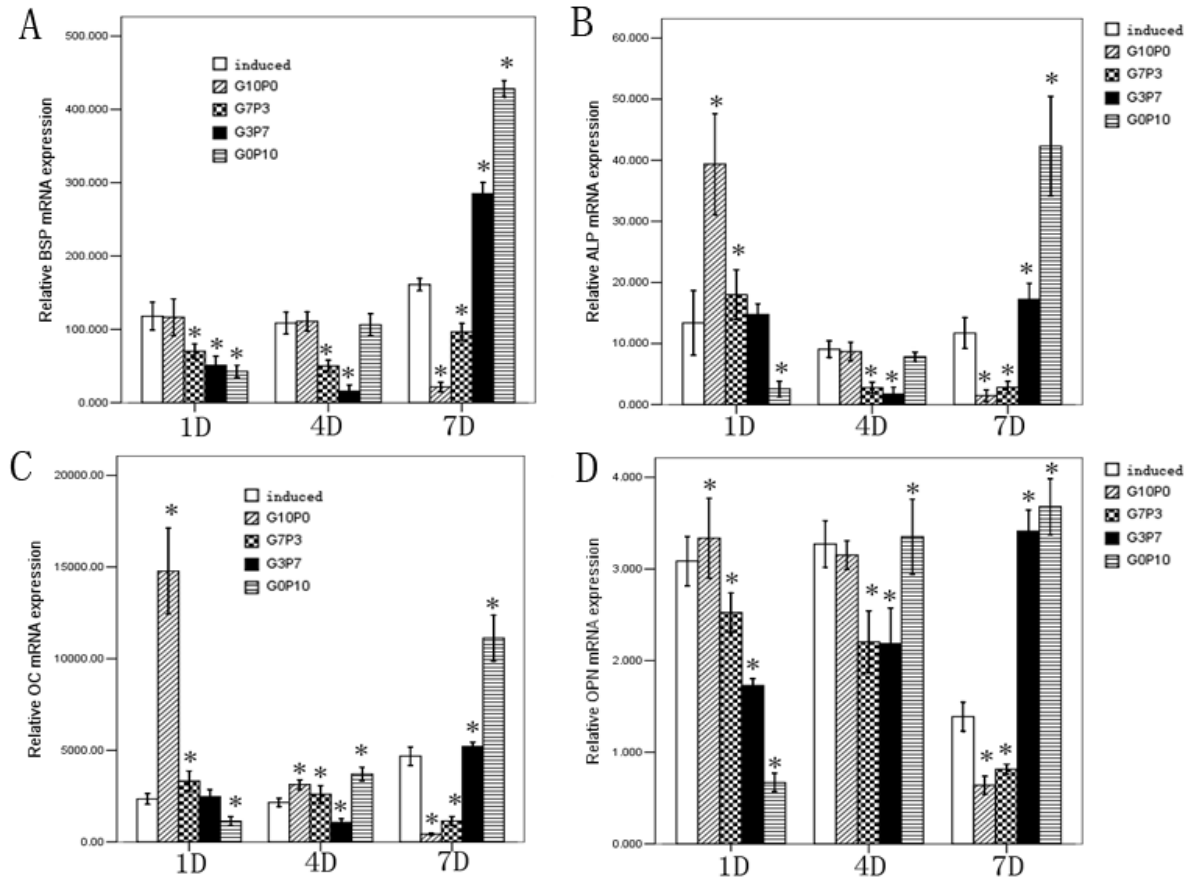
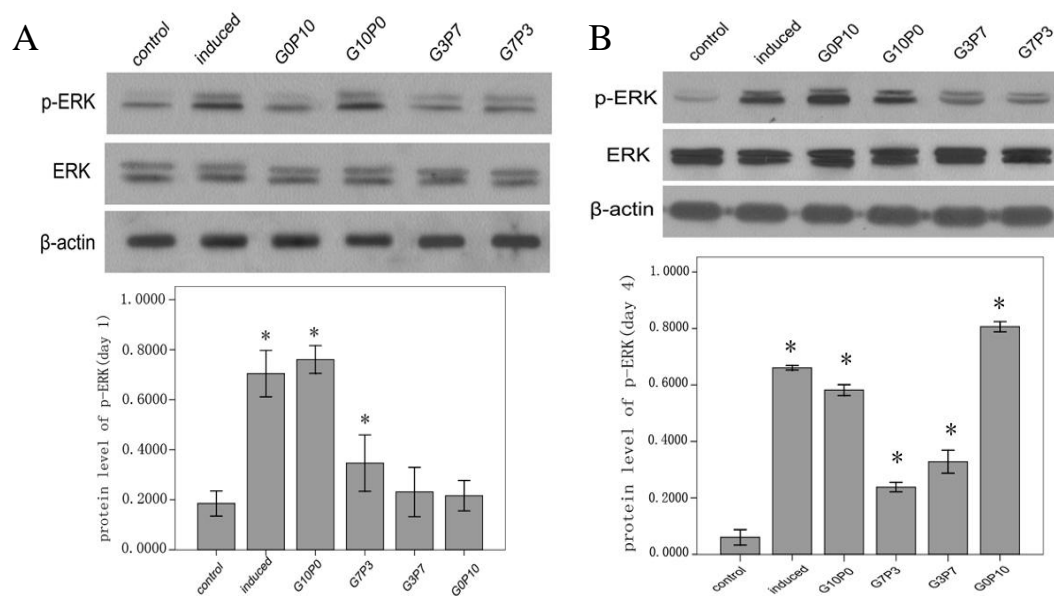


Figure 6 Real time-qPCR of osteogenic gene expression levels of mouse MSCs cultured in vitro. Total RNA was prepared from MSCs grown on either induced, G0P0, G7P3, G3P7, G0P10 groups for 1, 4 or 7 days. BSP(A), ALP(B), OC(C), OPN(D) gene expression was quantified using real time-qPCR methods, GAPDH was used as an internal control. Data values are expressed as mean \pm SE (n=3). “*” means $p < 0.05$ vs the induced group. .

4.7 Involvement of ERK1/2 activation in membranes that promote osteogenesis

Western blot analysis was performed to determine whether the ERK1/2 pathway was responsible for the increased osteogenesis stimulated by different nano-membranes. As shown in Figure 7, the G10P0 group exhibited the highest expression of phosphorylated ERK1/2 on day 1 and the activation of ERK1/2 showed a decreased trend from G10P0 group to G0P10 group on day 1 (Figure 6A). The activation of ERK1/2 in G0P10 group was increased on day 4 and sustained for 7 days. (Figure 6B, C). The activation of ERK1/2 showed a increased trend from G10P0 group to G0P10 group on day 7 (Figure 6C).



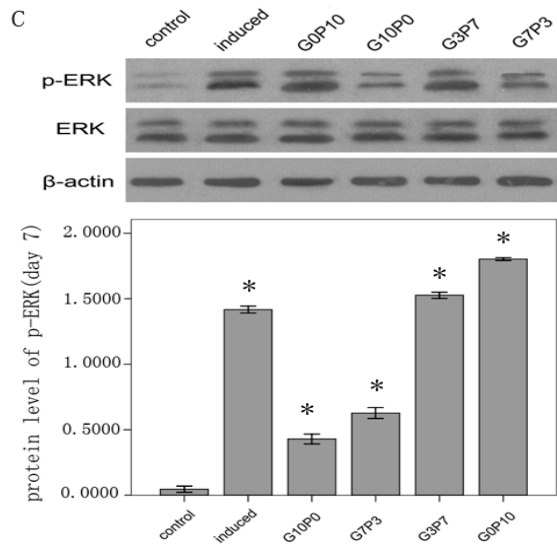


Figure 7 Western blot analysis of p-ERK protein expression in mouse MSCs. Total protein was prepared from MSC grown on either induced, G0P0, G7P3, G3P7, G0P10 for one(A), four(B) or seven(C) days. β -actin was used as an internal control. Data values are expressed as mean \pm SE (n=3). “*” means $p < 0.05$ vs the control group.

4.8 The relationship between MSCs' osteogenic differentiation on different nano-membrane

Bone marrow mesenchymal stem cells (MSCs) have been reported with the potential to differentiate into a variety of cell types both *in vivo* and *in vitro*. As for bone tissue engineering, MSCs have been proven to differentiate into an osteogenic lineage and have been widely used in bone tissue engineering as seed cells [119]. We used quantitative PCR to study the gene expression of a differentiation marker of osteoblasts in MSCs in three groups. The commitment of MSCs to osteogenic differentiation was demonstrated by the expression of BSP, ALP, OC and OPN. These proteins are considered as lineage-specific markers of osteoblastic differentiation. Bone sialoprotein(BSP) is a highly sulfated, phosphorylated, and glycosylated protein that mediates cell attachment through a RGD motif to extracellular matrices[120]. Due to its highly negative charge, BSP can sequester calcium ions while conserving polyglutamate regions, which have hydroxyapatite crystal nucleation potential[121]. In the absence of osteocalcin, bone sialoprotein could contribute to an overall metabolic shift toward new bone formation [122, 123]. Alkaline phosphatase (ALP) is an enzyme present in all tissue in the human body that removes the phosphate group. However, it is concentrated in bone and a high level of ALP may indicate active bone formation occurring, which makes it a marker for bone metabolism.[124]. Osteocalcin (OC) is a critical marker in late bone differentiation [125]. Osteopontin is a phosphoprotein member of the SIBLING family that possesses several calcium- binding domains and is associated with cell attachment, proliferation, and mineralization of extracellular matrix into bone, synthesized by bone-forming cells [126].

In the present study, four osteogenic genes expression results suggest that the fate of stem cells on membranes can be affected by the different composition of gelatin and PCL.

Gelatin can elicit osteogenic expression of MSCs at an early stage, but the PCL can elicit the osteogenic differentiation at a late stage.

4.9 Nano-membrane stimulation of MSCs' osteogenic differentiation through ERK1/2 signaling pathways

The differentiation of MSCs into osteoblasts is primarily controlled by Cbfa1/Runx2 [127]. Cbfa1/Runx2 phosphorylation and activation is mediated by ERK1/2 [128]. The activation of ERK1/2 has been demonstrated by studies to be involved in MSCs and osteoblast differentiation in response to various mechanical stimuli, including shock wave, hydrostatic pressure, fluid flow and cyclic strain[129-132]. Moreover, ERK1/2 activation is also associated with collagen synthesis, bone specific protein production and calcium deposition [129-133].

Stem cell differentiation has recently become increasingly linked to mechanobiological concepts such as cell-generated physical forces. These forces originate from myosin bundles sliding along actin filaments and are transmitted to the extracellular matrix (ECM), a three-dimensional fibrillar protein scaffold which surrounds and anchors cells. Transduction of these signals employs a vast array of adhesive proteins that assemble together to mechanically link the extracellular and intracellular worlds [134]. Integrins are receptors that mediate the attachment between a cell and the tissues that surround it, such as other cells or the ECM. Integrins have close relationship with the ERK1/2 activation. Mechanical strain promotes the proliferation of osteoblast cells via ERK mediation through integrins $\beta 1$ and $\beta 5$ [135], which may suggest that ERK1/2 is an essential pathway in the mechanotransduction process. We therefore hypothesized that ERK1/2 activation may also play an essential role in nano-membrane mediated-MSCs osteodifferentiation. Our results show that together with high osteogenic expression in certain nano-membranes, the ERK1/2 activation was significantly greater at the same time point, suggesting that via ERK1/2 pathway, nano-membranes stimulate MSCs osteodifferentiation.

Chapter V: Conclusions and Future Studies

A series of surfaces with different levels of hydrophilicity / hydrophobicity (or wettability) were fabricated by changing the ratio of gelatin and PCL content in a series of electrospun nanofibrous membranes. Measurements of the contact angle of water confirmed the gradient change of the surface wettabilities. The chemical structure of the gelatin/PCL (GP) composite nanofibrous membranes was characterized using FT-IR spectroscopy. From the *in vitro* degradation tests in PBS and cell culture medium which assessed the differential weight change, it was evident that the nanofibrous membranes were not degraded or eroded to a significant extent by either of the solution over a period of 7 days, which allowed for further cell culture and gene expression studies. MSCs were selected to be seeded onto the scaffolds and cell morphology and viability were evaluated using SEM, a live/dead staining assay as well as by an MTT assay. The nanofibrous membranes with different surface wettabilities had a significant influence on the cell motility, in which more hydrophilic surfaces were found to be more favorable for cell adhesion and spreading. The expression of genes associated with osteogenesis, including BSP, ALP, OPN and OC, were measured by real-time RT-PCR at different time points. It was found that the trend from G10P0 to G0P10 revealed a decreased trend in osteogenesis expression on day 1 and the trend from G10P0 to G0P10 showed an increased trend in osteogenesis expression by day 7. Then western blot analysis was performed to determine whether the ERK1/2 pathway was responsible for the different nano-membranes stimulating increased osteogenesis. The results suggested that ERK1/2 is an essential pathway in this mechanotransduction process. Our results showed that together with a high osteogenic

expression in the nano-membranes, ERK1/2 activation caused a significant increase at the same time point, suggesting that it was via the ERK1/2 pathway that the nano-membranes stimulate MSCs osteodifferentiation.

This discovery is striking namely that cell adhesion and growth as well as regulated differentiation is strongly associated with surface wettability. In the future, additional evidence is required to prove the significance of the ERK1/2 pathway in the mechanotransduction process. Since the gelatin/PCL nanofibrous membranes possess excellent biocompatibility and low cytotoxicity, *in vivo* experiments would appear to be imperative. If as hypothesized that level of surface wettability can perform therapeutic functions of specifically guiding differentiation and strong osseointegration for new bone tissue growth and development, it can be foreseen that the results can be significant for the further study of stem cell control and implant development, as well as its application to a therapeutic platform.

References

1. Phillips, J.E., et al., Human mesenchymal stem cell differentiation on self-assembled monolayers presenting different surface chemistries. *Acta Biomater*, 2010. **6**(1): p. 12-20.
2. Erickson, G.R., et al., Chondrogenic potential of adipose tissue-derived stromal cells in vitro and in vivo. *Biochem Biophys Res Commun*, 2002. **290**(2): p. 763-9.
3. Guo, W.H., et al., Substrate rigidity regulates the formation and maintenance of tissues. *Biophys J*, 2006. **90**(6): p. 2213-20.
4. Saha, K., et al., Substrate modulus directs neural stem cell behavior. *Biophys J*, 2008. **95**(9): p. 4426-38.
5. Neves, S.R., et al., Cell shape and negative links in regulatory motifs together control spatial information flow in signaling networks. *Cell*, 2008. **133**(4): p. 666-80.
6. Gerlach, J.C. and K. Zeilinger, Adult stem cell technology--prospects for cell based therapy in regenerative medicine. *Int J Artif Organs*, 2002. **25**(2): p. 83-90.
7. Lutolf, M.P. and J.A. Hubbell, Synthetic biomaterials as instructive extracellular microenvironments for morphogenesis in tissue engineering. *Nat Biotechnol*, 2005. **23**(1): p. 47-55.
8. Funayama, K., et al., An evidence for adhesion-mediated acquisition of acute myeloid leukemic stem cell-like immaturities. *Biochem Biophys Res Commun*, 2010. **392**(3): p. 271-6.
9. Desai, S.S., S.A. Kale, and S.G. Rao, Demonstration of a haemopoietic pluripotent stem cell adhesion molecule (HPSC-CAM) in mouse bone marrow. *Cell Biol Int Rep*, 1991. **15**(10): p. 929-42.
10. de Rooij, D.G., S. Repping, and A.M. van Pelt, Role for adhesion molecules in the

spermatogonial stem cell niche. *Cell Stem Cell*, 2008. **3**(5): p. 467-8.

11. Elhasid, R. and J.M. Rowe, Hematopoietic stem cell transplantation in neutrophil disorders: severe congenital neutropenia, leukocyte adhesion deficiency and chronic granulomatous disease. *Clin Rev Allergy Immunol*, 2010. **38**(1): p. 61-7.

12. Yamashita, Y.M., Cell adhesion in regulation of asymmetric stem cell division. *Curr Opin Cell Biol*, 2010. **22**(5): p. 605-10.

13. Lapidot, T. and I. Petit, Current understanding of stem cell mobilization: the roles of chemokines, proteolytic enzymes, adhesion molecules, cytokines, and stromal cells. *Exp Hematol*, 2002. **30**(9): p. 973-81.

14. Bruder, S.P., et al., Mesenchymal stem cell surface antigen SB-10 corresponds to activated leukocyte cell adhesion molecule and is involved in osteogenic differentiation. *J Bone Miner Res*, 1998. **13**(4): p. 655-63.

15. Arai, F., et al., Mesenchymal stem cells in perichondrium express activated leukocyte cell adhesion molecule and participate in bone marrow formation. *J Exp Med*, 2002. **195**(12): p. 1549-63.

16. Salto, C., et al., Control of neural stem cell adhesion and density by an electronic polymer surface switch. *Langmuir*, 2008. **24**(24): p. 14133-8.

17. Berrier, A.L. and K.M. Yamada, Cell-matrix adhesion. *J Cell Physiol*, 2007. **213**(3): p. 565-73.

18. Engler, A.J., et al., Matrix elasticity directs stem cell lineage specification. *Cell*, 2006. **126**(4): p. 677-89.

19. Burdick, J.A. and G. Vunjak-Novakovic, Engineered microenvironments for controlled stem cell differentiation. *Tissue Eng Part A*, 2009. **15**(2): p. 205-19.

20. Benoit, D.S., et al., Small functional groups for controlled differentiation of hydrogel-encapsulated human mesenchymal stem cells. *Nat Mater*, 2008. **7**(10): p. 816-23.
21. Brodbeck, W.G., et al., Biomaterial adherent macrophage apoptosis is increased by hydrophilic and anionic substrates in vivo. *Proc Natl Acad Sci U S A*, 2002. **99**(16): p. 10287-92.
22. Jiang, J. and E.T. Papoutsakis, Stem-Cell Niche Based Comparative Analysis of Chemical and Nano-mechanical Material Properties Impacting Ex Vivo Expansion and Differentiation of Hematopoietic and Mesenchymal Stem Cells. *Adv Healthc Mater*, 2012.
23. Huang, A.H., et al., Long-term dynamic loading improves the mechanical properties of chondrogenic mesenchymal stem cell-laden hydrogel. *Eur Cell Mater*, 2010. **19**: p. 72-85.
24. Murphy, C.M., et al., Mesenchymal stem cell fate is regulated by the composition and mechanical properties of collagen-glycosaminoglycan scaffolds. *J Mech Behav Biomed Mater*, 2012. **11**: p. 53-62.
25. Li, C.H., et al., Correlation between compositional and mechanical properties of human mesenchymal stem cell-collagen microspheres during chondrogenic differentiation. *Tissue Eng Part A*, 2011. **17**(5-6): p. 777-88.
26. Naito, H., et al., The effect of mesenchymal stem cell osteoblastic differentiation on the mechanical properties of engineered bone-like tissue. *Tissue Eng Part A*, 2011. **17**(17-18): p. 2321-9.
27. Mathieu, P.S. and E.G. Lobo, Cytoskeletal and focal adhesion influences on mesenchymal stem cell shape, mechanical properties, and differentiation down osteogenic, adipogenic, and chondrogenic pathways. *Tissue Eng Part B Rev*, 2012. **18**(6): p. 436-44.
28. Ayala, R., et al., Engineering the cell-material interface for controlling stem cell adhesion, migration, and differentiation. *Biomaterials*, 2011. **32**(15): p. 3700-11.

29. Lecuit, T. and P.F. Lenne, Cell surface mechanics and the control of cell shape, tissue patterns and morphogenesis. *Nat Rev Mol Cell Biol*, 2007. **8**(8): p. 633-44.
30. Liotta, L.A. and E.C. Kohn, The microenvironment of the tumour-host interface. *Nature*, 2001. **411**(6835): p. 375-9.
31. Chen, Y.M., et al., Tuning of cell proliferation on tough gels by critical charge effect. *J Biomed Mater Res A*, 2009. **88**(1): p. 74-83.
32. Stevens, M.M. and J.H. George, Exploring and engineering the cell surface interface. *Science*, 2005. **310**(5751): p. 1135-8.
33. Dalby, M.J., et al., The control of human mesenchymal cell differentiation using nanoscale symmetry and disorder. *Nat Mater*, 2007. **6**(12): p. 997-1003.
34. Dill, K.A., Dominant forces in protein folding. *Biochemistry*, 1990. **29**(31): p. 7133-55.
35. Kauzmann, W., Some factors in the interpretation of protein denaturation. *Adv Protein Chem*, 1959. **14**: p. 1-63.
36. Keselowsky, B.G., D.M. Collard, and A.J. Garcia, Integrin binding specificity regulates biomaterial surface chemistry effects on cell differentiation. *Proc Natl Acad Sci U S A*, 2005. **102**(17): p. 5953-7.
37. Liu, Z.J., Y. Zhuge, and O.C. Velazquez, Trafficking and differentiation of mesenchymal stem cells. *J Cell Biochem*, 2009. **106**(6): p. 984-91.
38. Tae, S.K., et al., Mesenchymal stem cells for tissue engineering and regenerative medicine. *Biomed Mater*, 2006. **1**(2): p. 63-71.
39. Daley, G.Q. and D.T. Scadden, Prospects for stem cell-based therapy. *Cell*, 2008. **132**(4): p. 544-8.
40. Assady, S., Challenges and prospects for stem cell-based therapy in diabetes mellitus. *Isr*

Med Assoc J, 2009. **11**(4): p. 212-5.

41. Scadden, D.T., The stem-cell niche as an entity of action. *Nature*, 2006. **441**(7097): p. 1075-9.
42. Morrison, S.J. and A.C. Spradling, Stem cells and niches: mechanisms that promote stem cell maintenance throughout life. *Cell*, 2008. **132**(4): p. 598-611.
43. Bobis, S., D. Jarocha, and M. Majka, Mesenchymal stem cells: characteristics and clinical applications. *Folia Histochem Cytobiol*, 2006. **44**(4): p. 215-30.
44. Discher, D.E., D.J. Mooney, and P.W. Zandstra, Growth factors, matrices, and forces combine and control stem cells. *Science*, 2009. **324**(5935): p. 1673-7.
45. Pittenger, M.F. and B.J. Martin, Mesenchymal stem cells and their potential as cardiac therapeutics. *Circ Res*, 2004. **95**(1): p. 9-20.
46. Abbott, J. and H. Holtzer, The loss of phenotypic traits by differentiated cells. 3. The reversible behavior of chondrocytes in primary cultures. *J Cell Biol*, 1966. **28**(3): p. 473-87.
47. Adams, G.B. and D.T. Scadden, A niche opportunity for stem cell therapeutics. *Gene Ther*, 2008. **15**(2): p. 96-9.
48. Daley, W.P., S.B. Peters, and M. Larsen, Extracellular matrix dynamics in development and regenerative medicine. *J Cell Sci*, 2008. **121**(Pt 3): p. 255-64.
49. Lopez-Juarez, A., et al., Thyroid hormone signaling acts as a neurogenic switch by repressing Sox2 in the adult neural stem cell niche. *Cell Stem Cell*, 2012. **10**(5): p. 531-43.
50. Wagers, A.J., The stem cell niche in regenerative medicine. *Cell Stem Cell*, 2012. **10**(4): p. 362-9.
51. Gomez-Gaviro, M.V., et al., The vascular stem cell niche. *J Cardiovasc Transl Res*, 2012. **5**(5): p. 618-30.

52. Murry, C.E. and G. Keller, Differentiation of embryonic stem cells to clinically relevant populations: Lessons from embryonic development. *Cell*, 2008. **132**(4): p. 661-680.
53. Gerecht, S., et al., Hyaluronic acid hydrogel for controlled self-renewal and differentiation of human embryonic stem cells. *Proc Natl Acad Sci U S A*, 2007. **104**(27): p. 11298-303.
54. Parmar, K., et al., Distribution of hematopoietic stem cells in the bone marrow according to regional hypoxia. *Proc Natl Acad Sci U S A*, 2007. **104**(13): p. 5431-6.
55. Schugar, R.C., P.D. Robbins, and B.M. Deasy, Small molecules in stem cell self-renewal and differentiation. *Gene Ther*, 2008. **15**(2): p. 126-35.
56. Xu, Y., Y. Shi, and S. Ding, A chemical approach to stem-cell biology and regenerative medicine. *Nature*, 2008. **453**(7193): p. 338-44.
57. Khan, M.R., et al., The enhanced modulation of key bone matrix components by modified Titanium implant surfaces. *Bone*, 2012. **50**(1): p. 1-8.
58. Kihara, T., et al., Exogenous type I collagen facilitates osteogenic differentiation and acts as a substrate for mineralization of rat marrow mesenchymal stem cells in vitro. *Biochemical and Biophysical Research Communications*, 2006. **341**(4): p. 1029-1035.
59. Choi, Y.J., et al., Alpha-adrenergic blocker mediated osteoblastic stem cell differentiation. *Biochem Biophys Res Commun*, 2011. **416**(3-4): p. 232-8.
60. Flaim, C.J., S. Chien, and S.N. Bhatia, An extracellular matrix microarray for probing cellular differentiation. *Nat Methods*, 2005. **2**(2): p. 119-25.
61. Soen, Y., et al., Exploring the regulation of human neural precursor cell differentiation using arrays of signaling microenvironments. *Mol Syst Biol*, 2006. **2**: p. 37.
62. Derda, R., et al., Defined substrates for human embryonic stem cell growth identified

from surface arrays. *ACS Chem Biol*, 2007. **2**(5): p. 347-55.

63. Chai, C. and K.W. Leong, Biomaterials approach to expand and direct differentiation of stem cells. *Mol Ther*, 2007. **15**(3): p. 467-80.

64. Saha, K., et al., Designing synthetic materials to control stem cell phenotype. *Curr Opin Chem Biol*, 2007. **11**(4): p. 381-7.

65. Chambers, S.M., et al., Highly efficient neural conversion of human ES and iPS cells by dual inhibition of SMAD signaling. *Nat Biotechnol*, 2009. **27**(3): p. 275-80.

66. McLean, A.B., et al., Activin efficiently specifies definitive endoderm from human embryonic stem cells only when phosphatidylinositol 3-kinase signaling is suppressed. *Stem Cells*, 2007. **25**(1): p. 29-38.

67. Borowiak, M., et al., Small molecules efficiently direct endodermal differentiation of mouse and human embryonic stem cells. *Cell Stem Cell*, 2009. **4**(4): p. 348-58.

68. Zaruba, M.M., et al., Synergy between CD26/DPP-IV inhibition and G-CSF improves cardiac function after acute myocardial infarction. *Cell Stem Cell*, 2009. **4**(4): p. 313-23.

69. North, T.E., et al., Prostaglandin E2 regulates vertebrate haematopoietic stem cell homeostasis. *Nature*, 2007. **447**(7147): p. 1007-11.

70. Folkman, J. and A. Moscona, Role of cell shape in growth control. *Nature*, 1978. **273**(5661): p. 345-9.

71. Manasek, F.J., M.B. Burnside, and R.E. Waterman, Myocardial cell shape change as a mechanism of embryonic heart looping. *Dev Biol*, 1972. **29**(4): p. 349-71.

72. Ingber, D., Extracellular matrix and cell shape: potential control points for inhibition of angiogenesis. *J Cell Biochem*, 1991. **47**(3): p. 236-41.

73. Holtzer, H., et al., The Loss of Phenotypic Traits by Differentiated Cells in Vitro, I.

- Dedifferentiation of Cartilage Cells. *Proc Natl Acad Sci U S A*, 1960. **46**(12): p. 1533-42.
74. Benya, P.D. and J.D. Shaffer, Dedifferentiated chondrocytes reexpress the differentiated collagen phenotype when cultured in agarose gels. *Cell*, 1982. **30**(1): p. 215-24.
75. Hoben, G.M., E.J. Koay, and K.A. Athanasiou, Fibrochondrogenesis in two embryonic stem cell lines: effects of differentiation timelines. *Stem Cells*, 2008. **26**(2): p. 422-30.
76. Johnstone, B., et al., In vitro chondrogenesis of bone marrow-derived mesenchymal progenitor cells. *Exp Cell Res*, 1998. **238**(1): p. 265-72.
77. McBride, S.H. and M.L. Knothe Tate, Modulation of stem cell shape and fate A: the role of density and seeding protocol on nucleus shape and gene expression. *Tissue Eng Part A*, 2008. **14**(9): p. 1561-72.
78. Hwang, N.S., et al., Effects of three-dimensional culture and growth factors on the chondrogenic differentiation of murine embryonic stem cells. *Stem Cells*, 2006. **24**(2): p. 284-91.
79. Awad, H.A., et al., Chondrogenic differentiation of adipose-derived adult stem cells in agarose, alginate, and gelatin scaffolds. *Biomaterials*, 2004. **25**(16): p. 3211-22.
80. Meyers, J., J. Craig, and D.J. Odde, Potential for control of signaling pathways via cell size and shape. *Curr Biol*, 2006. **16**(17): p. 1685-93.
81. Guilak, F., A. Ratcliffe, and V.C. Mow, Chondrocyte deformation and local tissue strain in articular cartilage: a confocal microscopy study. *J Orthop Res*, 1995. **13**(3): p. 410-21.
82. Ingber, D.E., The mechanochemical basis of cell and tissue regulation. *Mech Chem Biosyst*, 2004. **1**(1): p. 53-68.
83. Hwang, N.S., et al., Chondrogenic differentiation of human embryonic stem cell-derived cells in arginine-glycine-aspartate-modified hydrogels. *Tissue Eng*, 2006. **12**(9): p. 2695-706.
84. Kloxin, A.M., et al., Photodegradable hydrogels for dynamic tuning of physical and

chemical properties. *Science*, 2009. **324**(5923): p. 59-63.

85. Emerman, J.T., S.J. Burwen, and D.R. Pitelka, Substrate properties influencing ultrastructural differentiation of mammary epithelial cells in culture. *Tissue Cell*, 1979. **11**(1): p. 109-19.
86. Kurpinski, K., et al., Anisotropic mechanosensing by mesenchymal stem cells. *Proc Natl Acad Sci U S A*, 2006. **103**(44): p. 16095-100.
87. Pelham, R.J., Jr. and Y. Wang, Cell locomotion and focal adhesions are regulated by substrate flexibility. *Proc Natl Acad Sci U S A*, 1997. **94**(25): p. 13661-5.
88. Wang, H.B., M. Dembo, and Y.L. Wang, Substrate flexibility regulates growth and apoptosis of normal but not transformed cells. *Am J Physiol Cell Physiol*, 2000. **279**(5): p. C1345-50.
89. Hadjipanayi, E., V. Mudera, and R.A. Brown, Close dependence of fibroblast proliferation on collagen scaffold matrix stiffness. *J Tissue Eng Regen Med*, 2009. **3**(2): p. 77-84.
90. Deroanne, C.F., C.M. Lapiere, and B.V. Nussgens, In vitro tubulogenesis of endothelial cells by relaxation of the coupling extracellular matrix-cytoskeleton. *Cardiovasc Res*, 2001. **49**(3): p. 647-58.
91. Engler, A.J., et al., Myotubes differentiate optimally on substrates with tissue-like stiffness: pathological implications for soft or stiff microenvironments. *J Cell Biol*, 2004. **166**(6): p. 877-87.
92. Winer, J.P., et al., Bone marrow-derived human mesenchymal stem cells become quiescent on soft substrates but remain responsive to chemical or mechanical stimuli. *Tissue Eng Part A*, 2009. **15**(1): p. 147-54.

93. Berry, M.F., et al., Mesenchymal stem cell injection after myocardial infarction improves myocardial compliance. *Am J Physiol Heart Circ Physiol*, 2006. **290**(6): p. H2196-203.
94. Sinha, D.N., P.C. Gupta, and G. P, Tobacco use among students and school personnel in India. *Asian Pac J Cancer Prev*, 2007. **8**(3): p. 417-21.
95. Pitchford, S.C., et al., Differential mobilization of subsets of progenitor cells from the bone marrow. *Cell Stem Cell*, 2009. **4**(1): p. 62-72.
96. Wipff, P.J., et al., Myofibroblast contraction activates latent TGF-beta1 from the extracellular matrix. *J Cell Biol*, 2007. **179**(6): p. 1311-23.
97. Watt, F.M. and B.L. Hogan, Out of Eden: stem cells and their niches. *Science*, 2000. **287**(5457): p. 1427-30.
98. Nel, A., et al., Toxic potential of materials at the nanolevel. *Science*, 2006. **311**(5761): p. 622-7.
99. Oberdorster, G., et al., Principles for characterizing the potential human health effects from exposure to nanomaterials: elements of a screening strategy. *Part Fibre Toxicol*, 2005. **2**: p. 8.
100. Recknor, J.B., D.S. Sakaguchi, and S.K. Mallapragada, Directed growth and selective differentiation of neural progenitor cells on micropatterned polymer substrates. *Biomaterials*, 2006. **27**(22): p. 4098-108.
101. Yim, E.K., S.W. Pang, and K.W. Leong, Synthetic nanostructures inducing differentiation of human mesenchymal stem cells into neuronal lineage. *Exp Cell Res*, 2007. **313**(9): p. 1820-9.
102. Arnold, M., et al., Activation of integrin function by nanopatterned adhesive interfaces. *ChemPhysChem*, 2004. **5**(3): p. 383-8.

103. Gerecht, S., et al., The effect of actin disrupting agents on contact guidance of human embryonic stem cells. *Biomaterials*, 2007. **28**(28): p. 4068-77.
104. Nel, A.E., et al., Understanding biophysicochemical interactions at the nano-bio interface. *Nat Mater*, 2009. **8**(7): p. 543-57.
105. Ma, Z.W., M. Kotaki, and S. Ramakrishna, Surface modified nonwoven polysulphone (PSU) fiber mesh by electrospinning: A novel affinity membrane. *Journal of Membrane Science*, 2006. **272**(1-2): p. 179-187.
106. Heydarkhan-Hagvall, S., et al., Three-dimensional electrospun ECM-based hybrid scaffolds for cardiovascular tissue engineering. *Biomaterials*, 2008. **29**(19): p. 2907-2914.
107. Song, J.-H., H.-E. Kim, and H.-W. Kim, Electrospun fibrous web of collagen–apatite precipitated nanocomposite for bone regeneration. *Journal of Materials Science: Materials in Medicine*, 2008. **19**(8): p. 2925-2932.
108. Hua, J., et al., Characterization of mesenchymal stem cells (MSCs) from human fetal lung: potential differentiation of germ cells. *Tissue Cell*, 2009. **41**(6): p. 448-55.
109. Ackerman, S.J., M.S. Mafilios, and D.W. Polly, Jr., Economic evaluation of bone morphogenetic protein versus autogenous iliac crest bone graft in single-level anterior lumbar fusion: an evidence-based modeling approach. *Spine (Phila Pa 1976)*, 2002. **27**(16 Suppl 1): p. S94-9.
110. Lin, Y., et al., Surface modification of poly(L-lactic acid) to improve its cytocompatibility via assembly of polyelectrolytes and gelatin. *Acta Biomater*, 2006. **2**(2): p. 155-64.
111. Kagami, H., H. Agata, and A. Tojo, Bone marrow stromal cells (bone marrow-derived multipotent mesenchymal stromal cells) for bone tissue engineering: basic science to clinical

translation. *Int J Biochem Cell Biol*, 2011. **43**(3): p. 286-9.

112. Mouthuy, P.A., et al., Physico-chemical characterization of functional electrospun scaffolds for bone and cartilage tissue engineering. *Proc Inst Mech Eng H*, 2010. **224**(12): p. 1401-14.

113. Venugopal, J.R., et al., Nanobioengineered electrospun composite nanofibers and osteoblasts for bone regeneration. *Artif Organs*, 2008. **32**(5): p. 388-97.

114. Skotak, M., et al., Improved cellular infiltration into nanofibrous electrospun cross-linked gelatin scaffolds templated with micrometer-sized polyethylene glycol fibers. *Biomedical Materials*, 2011. **6**(5).

115. Qian, Y.F., et al., Cross-linking of gelatin and chitosan complex nanofibers for tissue-engineering scaffolds. *J Biomater Sci Polym Ed*, 2011. **22**(8): p. 1099-113.

116. Chong, E.J., et al., Evaluation of electrospun PCL/gelatin nanofibrous scaffold for wound healing and layered dermal reconstitution. *Acta Biomater*, 2007. **3**(3): p. 321-30.

117. Zhang, Y.Z., et al., Electrospinning of gelatin fibers and gelatin/PCL composite fibrous scaffolds. *Journal of Biomedical Materials Research Part B-Applied Biomaterials*, 2005. **72B**(1): p. 156-165.

118. Zhang, Y.Z., et al., Fabrication of porous electrospun nanofibres. *Nanotechnology*, 2006. **17**(3): p. 901-908.

119. Yuan, J., et al., Repair of canine mandibular bone defects with bone marrow stromal cells and porous beta-tricalcium phosphate. *Biomaterials*, 2007. **28**(6): p. 1005-13.

120. Ganss, B., R.H. Kim, and J. Sodek, Bone sialoprotein. *Crit Rev Oral Biol Med*, 1999. **10**(1): p. 79-98.

121. Hunter, G.K. and H.A. Goldberg, Nucleation of hydroxyapatite by bone sialoprotein.

- Proc Natl Acad Sci U S A, 1993. **90**(18): p. 8562-5.
122. Hunter, G.K. and H.A. Goldberg, Modulation of crystal formation by bone phosphoproteins: role of glutamic acid-rich sequences in the nucleation of hydroxyapatite by bone sialoprotein. *Biochem J*, 1994. **302** (Pt 1): p. 175-9.
123. Kondo, H., et al., Temporal changes of mRNA expression of matrix proteins and parathyroid hormone and parathyroid hormone-related protein (PTH/PTHrP) receptor in bone development. *J Bone Miner Res*, 1997. **12**(12): p. 2089-97.
124. Aschaffenburg, R. and J.E.C. Mullen, 381. A rapid and simple phosphatase test for milk. *Journal of Dairy Research*, 1949. **16**(01): p. 58-67.
125. Chun, C., et al., The use of injectable, thermosensitive poly(organophosphazene)-RGD conjugates for the enhancement of mesenchymal stem cell osteogenic differentiation. *Biomaterials*, 2009. **30**(31): p. 6295-308.
126. Butler, W.T., The nature and significance of osteopontin. *Connect Tissue Res*, 1989. **23**(2-3): p. 123-36.
127. Ducy, P., et al., *Osf2/Cbfa1*: a transcriptional activator of osteoblast differentiation. *Cell*, 1997. **89**(5): p. 747-54.
128. Xiao, G., et al., Fibroblast growth factor 2 induction of the osteocalcin gene requires MAPK activity and phosphorylation of the osteoblast transcription factor, *Cbfa1/Runx2*. *J Biol Chem*, 2002. **277**(39): p. 36181-7.
129. Kim, S.H., et al., ERK 1/2 activation in enhanced osteogenesis of human mesenchymal stem cells in poly(lactic-glycolic acid) by cyclic hydrostatic pressure. *J Biomed Mater Res A*, 2007. **80**(4): p. 826-36.
130. Simmons, C.A., et al., Cyclic strain enhances matrix mineralization by adult human

mesenchymal stem cells via the extracellular signal-regulated kinase (ERK1/2) signaling pathway. J Biomech, 2003. **36**(8): p. 1087-96.

131. Wang, F.S., et al., Superoxide mediates shock wave induction of ERK-dependent osteogenic transcription factor (CBFA1) and mesenchymal cell differentiation toward osteoprogenitors. J Biol Chem, 2002. **277**(13): p. 10931-7.

132. Weyts, F.A., et al., ERK activation and alpha v beta 3 integrin signaling through Shc recruitment in response to mechanical stimulation in human osteoblasts. J Cell Biochem, 2002. **87**(1): p. 85-92.

133. Lai, C.F., et al., Erk is essential for growth, differentiation, integrin expression, and cell function in human osteoblastic cells. J Biol Chem, 2001. **276**(17): p. 14443-50.

134. Reilly, G.C. and A.J. Engler, Intrinsic extracellular matrix properties regulate stem cell differentiation. J Biomech, 2010. **43**(1): p. 55-62.

135. Yan, Y.X., et al., Mechanical strain regulates osteoblast proliferation through integrin-mediated ERK activation. PLoS One, 2012. **7**(4): p. e35709.